A CLIMATOLOGICAL ANALYSIS OF DROUGHT AND TORNADIC ACTIVITY IN THE SOUTHEASTERN UNITED STATES

by

THERESA KATE ANDERSEN

(Under the Direction of J. Marshall Shepherd)

ABSTRACT

The Intergovernmental Panel on Climate Change (IPCC) has indicated the probability of an acceleration of the water cycle due to climate change prompting more research on surface moisture feedbacks. Antecedent drought is hypothesized to reduce convection in the spring, possibly through soil moisture memory (forced by ridging) and subsequent atmospheric response. The relationship between Southeast tornadoes and drought is analyzed by quantifying the frequency of tornado day occurrence under antecedent drought conditions, understanding how antecedent drought is related to tornadic environments and the role of soil moisture memory, and determining if drought is influenced by the Bermuda High. Correlation analysis indicates fall/winter drought is associated with drought conditions in the spring, reduced convection, and below normal tornado activity. This research presents one of the first attempts to consider physical mechanisms that explain recent observational evidence of reduced tornado days following antecedent drought in the fall/winter seasons.

INDEX WORDS: Climate, Drought, Moisture recycling, Soil moisture memory, Tornadoes

A CLIMATOLOGICAL ANALYSIS OF DROUGHT AND TORNADIC ACTIVITY IN THE SOUTHEASTERN UNITED STATES

By

THERESA KATE ANDERSEN

B.S., Iowa State University, 2008

A Thesis Submitted to the Graduate Faculty of the University of Georgia in Partial Fulfillment of the Requirements for the Degree

MASTER OF SCIENCE

ATHENS, GEORGIA

2010

A CLIMATOLOGICAL ANALYSIS OF DROUGHT AND TORNADIC ACTIVITY

IN THE SOUTHEASTERN UNITED STATES

by

THERESA KATE ANDERSEN

Major Professor: J. Marshall Shepherd

Committee: Thomas L. Mote
Andrew J. Grundstein

Electronic Version Approved:

Maureen Grasso
Dean of the Graduate School
The University of Georgia
August 2010

ACKNOWLEDGEMENTS

I would like to thank my thesis committee members and especially my major professor, J. Marshall Shepherd. I came away from each meeting with him feeling 10 times more confident and happier with my research than I did before. I am lucky to have such a supportive advisor that eliminates the stress of graduate school. I would also like to thank my family and friends for their interest and support along the way. I acknowledge the NASA Water and Energy Cycle Program and Dr. Jared Entin for providing the funding for this research.

TABLE OF CONTENTS

LIST OF TABLES

PAGE

LIST OF FIGURES

PAGE

CHAPTER 1

INTRODUCTION

Land surface characteristics such as soil moisture have a direct effect on the atmosphere through moisture and energy exchanges. The moisture supply and instability of the planetary boundary layer (PBL) are key elements for convective storm development. Likewise, the lack of sufficient soil moisture has been speculated to reduce convective development and tornadoes in the spring. Global oceanic-atmospheric coupling has also been studied in relation to tornadic activity. Munoz and Enfield (2009) identify the March Pacific/North American teleconnection pattern (PNA) as having the highest correlation to tornadoes compared to other teleconnections. However, they primarily used a tornado count index which can be unreliable and inconsistent over long periods of time (Shepherd et al. 2009). El Niño Southern Oscillation (ENSO) phases have been linked to winter tornado activity in terms of influencing the location and strength of tornado outbreaks. ENSO refers to the ocean temperature oscillation in the Equatorial Pacific consisting of a cool phase (La Niña) and a warm phase (El Niño). These ocean temperature anomalies affect the atmospheric circulation and weather globally. During periods of neutral ENSO phases, tornado outbreaks in the southeastern United States tend to be more frequent than during El Niño. Tornado frequency during La Niña is greater than during El Niño, but less than during neutral phases. Of the three phases, Georgia experiences the most tornado occurrences during neutral ENSO winters (Fig. 1.1) (Cook and Schaefer 2008).

Shepherd et al. (2009) noted that studies such as Hagemeyer (1998) and Bove (1998) comparing ENSO and tornado activity show conflicting results and thus, there is no conclusive understanding of the relationship between tornado activity and ENSO. A different approach for analyzing the causes of suppressed tornado activity is essential. The Intergovernmental Panel on Climate Change (IPCC) has indicated the probability of an acceleration of the water cycle and increased frequency of hydroclimate anomalies due to climate change (Shepherd et al. 2009, Trenberth et al. 2007). Soil moisture fluxes influence the atmosphere and convection. Therefore, it is the intent of this study to analyze the relationship between the lack of soil moisture (e.g. drought) and tornadic activity. This research focuses on the southeastern United States where both drought and tornado occurrences are common. Soil moisture data provide an alternative approach to Shepherd et al. (2009), who used precipitation estimates, and may be used to calculate a new drought index.

1.1 Motivation

The consensus on soil moisture – atmospheric feedbacks is that surface heat fluxes and moisture gradients influence convective development. Soil has the capacity to hold moisture in small pores between particles. Gravitational water moves quickly downward through the pores to saturate deeper layers, while capillary water is held by soil particles against gravity. Soil moisture can evaporate into the air above the surface and thus provide moisture to the atmosphere. There is a lack of literature on the extension of soil moisture – atmospheric feedbacks to convective hazards such as tornado activity. Tornadoes are associated with deep, moist convection and the relationship between tornado activity and soil moisture by means of convection is important to study. Furthermore, the projections of increased frequency of extreme water cycle events highlight the need for further analysis of drought-severe weather relationships. Galway (1979) found a small trend for high-precipitation years to have more tornadoes than low-precipitation years, but he did not find that tornadoes were suppressed under drought conditions. Of his three study areas (southeastern United States, Great Plains, and Great Lakes), the Southeast had the greatest correlation between departure from normal precipitation and tornado occurrence (Fig. 1.2). However, the datasets Galway used are now outdated and spanned a time period when tornado counts were probably underestimated due to smaller populations and lack of Doppler radar networks (Shepherd et al. 2009). The study also focused on simultaneous rainfall and tornado activity over a short time and was limited to point-source rain gauge data to calculate the average seasonal rainfall. Raddatz and Cummine (2003) suggested that moisture fluxes from the Prairie agro-ecosystem may be associated with the seasonal pattern of tornado days. Hanesiak et al. (2009) continued that line of research and showed that soil moisture in the Canadian prairie could be a good predictor of severe convective weather (i.e. hail, tornadoes, heavy rains, or strong winds) in the warm season. A recent study by Shepherd et al. (2009) suggests that tornado activity in the spring is suppressed in north Georgia when meteorological drought occurred the previous fall and winter. Shortcomings of Shepherd et al. (2009) are that the study area is relatively limited in size and frequency of tornadic activity, the study is limited to one antecedent period, precipitation is used as a proxy for soil moisture, and physical mechanisms are not addressed. No other studies on the topic have been published to compare Galway's results. The large-scale water-cycle hazards associated with climate change have significant implications for rainfall patterns and future droughts, making it imperative to perform a climatological analysis on related feedbacks. The lack of consensus on ENSO-tornado connectivity further motivates research on this topic.

An analysis of the association between antecedent drought conditions and tornado activity has implications for seasonal forecasting and the future research of land-atmosphere feedbacks. Atlanta experienced deadly tornado outbreaks 14 March 2008 during a severe drought period. Therefore, it should be emphasized that tornadoes do occur during antecedent drought, but are hypothesized to be less frequent than during antecedent non-drought conditions. Fig. 1.3 (a) shows the Drought Monitor documented drought conditions for the Southeast during March 2008. Additionally, an analysis of Tropical Rainfall Measuring Mission-based rainfall anomalies for the period September 2007 to May 2008 reveals that parts of the Southeast were 0 to 80% below normal precipitation (Fig. 1.3 b). A map of the tornado tracks from the 2006-2008 drought period is provided (Fig. 1.4).

Galway (1979) and Shepherd et al. (2009) paved the way for drought-tornadic research and it is essential to continue the research using newer data and a different approach to yield more robust results. The March 2008 Atlanta tornado motivated further analysis of the role soil moisture plays in influencing tornadic environments. It is the intent of this study to investigate the relationship, if any, between southeastern United States tornadoes and drought.

1.2 Research Objectives

This research focuses on the following objectives:

1. Quantify the frequency of tornado occurrence under antecedent drought conditions in the Southeastern United States.
2. Understand how antecedent drought is related to physical mechanisms linked to tornado environments, specifically: Convective Available Potential Energy (CAPE), Convective Inhibition (CIN), and upper-level forcing.
3. Quantify soil moisture memory and analyze its relationship to potential tornadic activity.
4. Compare the soil moisture data to the Bermuda High Index (BHI) to determine if drought and BHI have any correlation.

The first research objective is to quantify the frequency of tornado occurrence under antecedent drought conditions in the southeastern United States. Tornado days are used to quantify occurrences instead of tornado counts for much of the analysis to reduce bias associated with extreme tornado outbreaks. Historical tornado data have issues related to changes in reporting style, population size, and new technology (Doswell and Burgess 1987, Grazulis 1993, Ashley 2007). It is hypothesized that tornado days and multiple tornado days are more (less) frequent under non-drought (drought) conditions. To determine drought, normalized monthly North American Regional Reanalysis (NARR) soil moisture data are compared to Palmer Drought Severity Index (PDSI) *Z*-index over six climate zones of the study area. This reveals how well the NARR soil moisture data captures drought over 1-, 2-, and 6-month antecedent periods to the tornado season. It is hypothesized that 6-month normalized soil moisture correlates to the *Z*-index more consistently than the shorter antecedent periods, as one or two months may not be long enough to capture a drought. Based on 6-month antecedent normalized soil moisture values, there are six drought years in the study period. Composite tornado track maps for the six drought years and six wettest years are compared to assess if soil moisture conditions correlate to the frequency and distribution of tornadoes. It is hypothesized that the drought composite tornado track map indicates fewer occurrence of tornadoes than the non-drought map as tornadoes are suppressed under fall/winter drought conditions.

The second objective is to understand how antecedent drought is related to physical mechanisms linked to tornadic environments (e.g. instability and upper-level forcing). CAPE and CIN 1-month antecedent to the tornado season are initially evaluated. It is hypothesized that drought is associated with lower CAPE and higher CIN environments due to weak surface sensible and latent heat fluxes corresponding to reduced soil moisture, unless recent rainfall is present to promote differential heating. CAPE and CIN composites during the tornado season are also utilized to assess the importance of the value ranges. Composite 1-month antecedent 500 hPa geopotential height maps for the six drought years and six wettest years are generated to assess the large-scale synoptic environment preceding the tornado season. It is hypothesized the drought years correlate to higher 500 hPa heights relative to Bermuda due to upper-level ridging.

The third objective is to quantify soil moisture memory, the persistence of soil moisture anomalies from fall/winter to spring. Fall/winter soil moisture is compared to spring values to determine any persistent patterns among drought, normal, and wet antecedent periods. It is hypothesized that soil moisture is more persistent from fall/winter to spring during drier conditions, as suggested by the literature on soil moisture memory.

The fourth objective is to calculate a Bermuda High Index (BHI) modified to the study area to determine if fall/winter drought and the Bermuda High are related. In the southeastern United States, it has been shown that the BHI strongly correlates with soil moisture deficits during the warm season as the Bermuda High influences both regional temperature and precipitation (Henderson and Vega 1996, Doublin and Grundstein 2008). Although the BHI index is categorized with oscillations such as the Pacific North American (PNA), the North Atlantic (NAO), and ENSO, it is not a teleconnection. The Bermuda High is a local phenomenon affecting the Atlantic and eastern United States. Teleconnections will not be explored in this thesis, but may be integrated into future research. It is hypothesized that the

1- and 6-month antecedent periods defined as drought years will be correlated to negative phases of the BHI.

These four objectives provide an understanding of the reliability of soil moisture data as a drought indicator, a tornado climatology and frequency of drought in the Southeast, the physical mechanisms linking drought and convection, soil moisture persistence on a seasonal scale, and the influence of the Bermuda High on drought conditions. Chapter 2 provides a review of the literature on these topics.

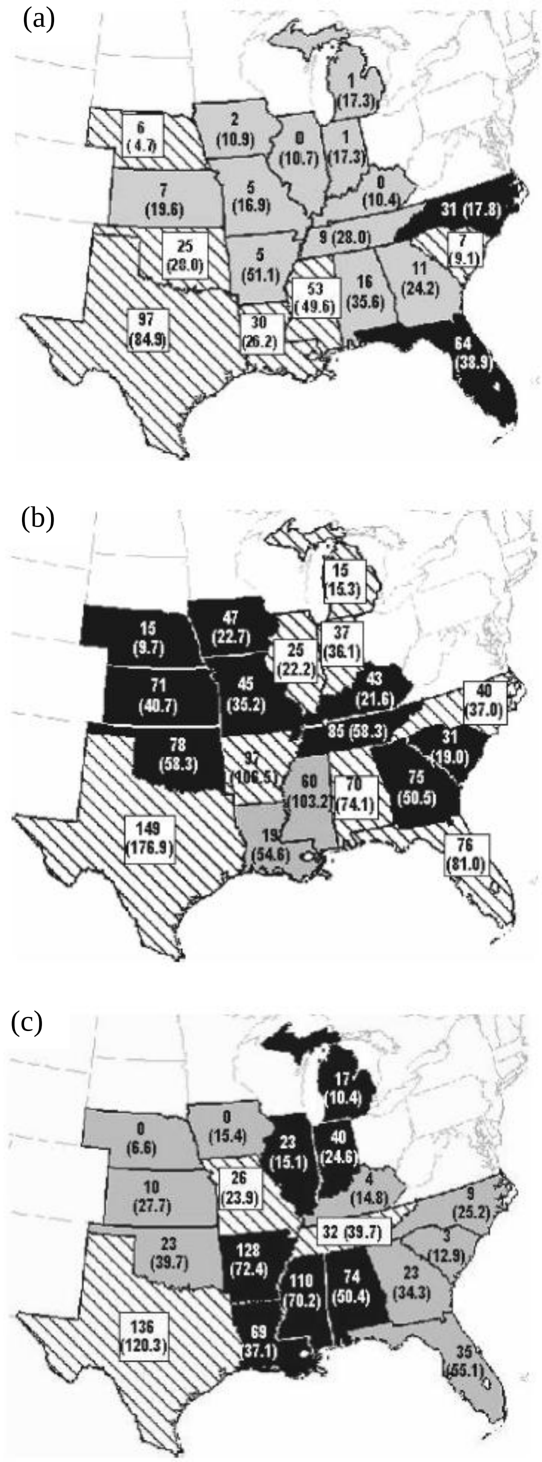

Fig. 1.1. Tornadoes occurring in winter during (a) El Niño, (b) Neutral ENSO, and (c) La Niña by state. The expected values independent of ENSO are in parentheses (from Cook and Schaefer 2008).

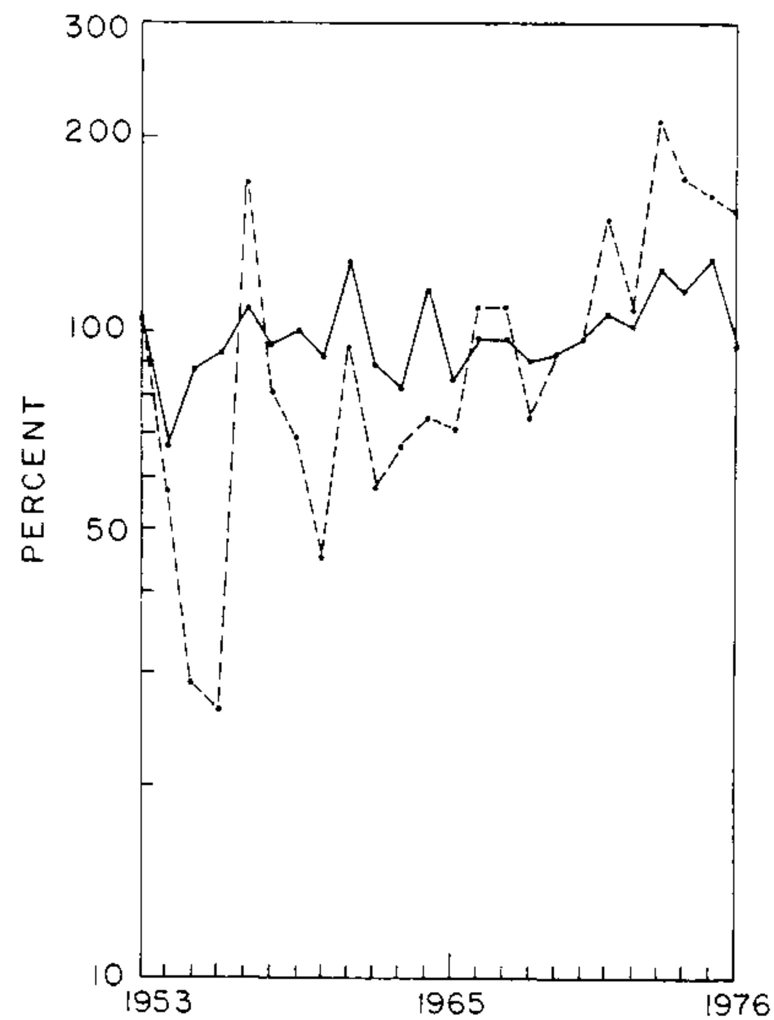

Fig. 1.2. Time series of the departure from normal of annual precipitation (solid) and tornado occurrence (dashed), 1953-1976 for the southeastern United States (from Galway 1979).

(a)

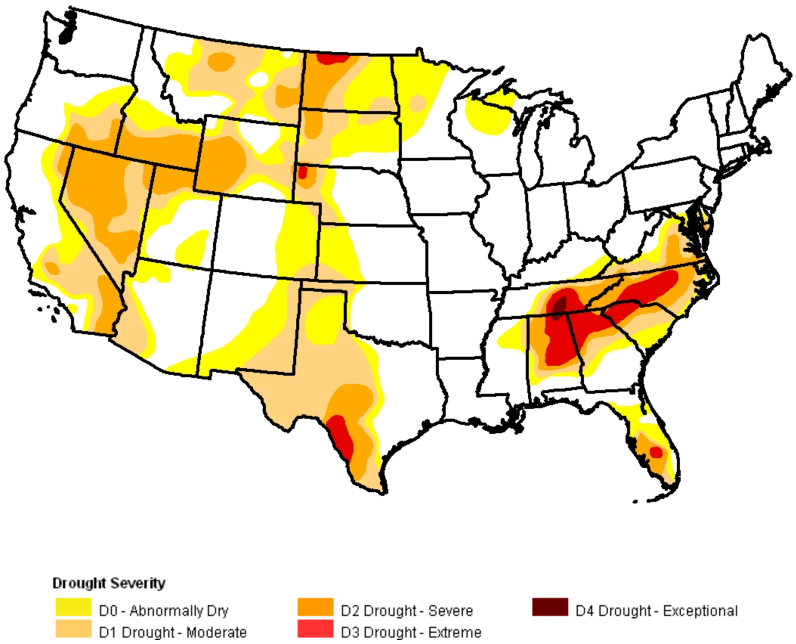

(b)

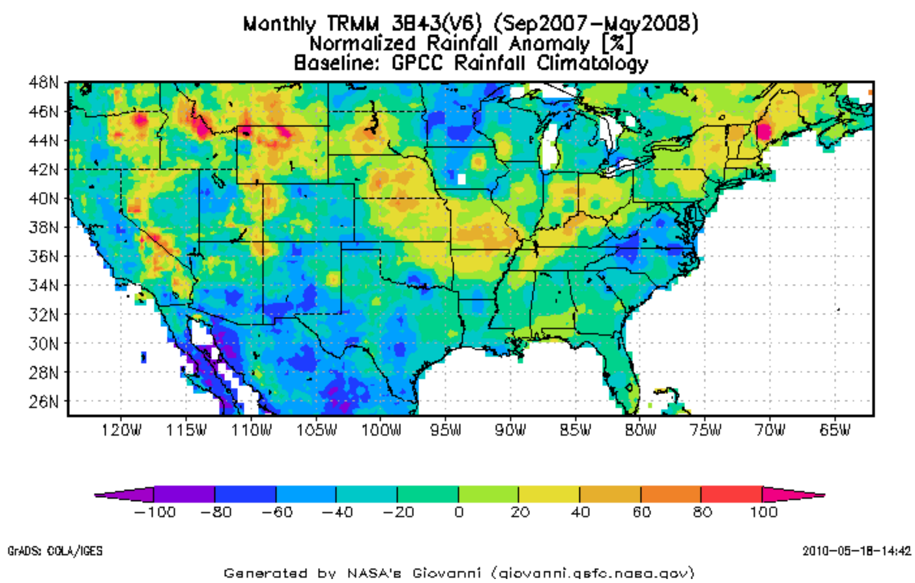

Fig. 1.3. (a) 14 March 2008 drought report from the U.S. Drought Monitor archives. Atlanta was in extreme drought conditions when the tornado outbreak occurred. (b) Normalized rainfall anomaly 2007 September to 2008 May using the Tropical Rainfall Measuring Mission Multi-Satellite Precipitation Analysis referenced to the Global Precipitation Climatology Center (GPCC) baseline.

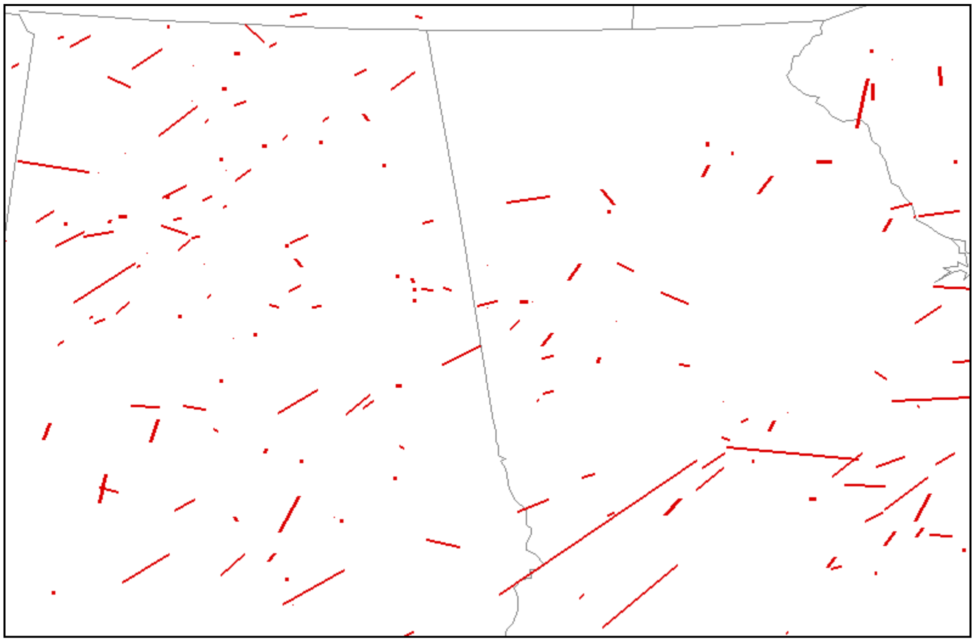

Fig. 1.4. SeverePlot tornado tracks over the southeastern United States during 2007-2008, a severe drought period.

CHAPTER 2

LITERATURE REVIEW

2.1 Drought

Several major drought periods are evident in the historical records during the previous half century. The 1954 drought was intense and spread from the Midwest to the south during the summer. In 1975, 1976, 1977, and 1980, drought plagued the southern Atlantic states. A persistent high pressure system over the southern Plains in 1980 caused a major heatwave considered to be the worst since 1954 and led to severe drought (Karl and Quayle 1981). Record drought occurred in the southeastern United States in 1986 due to dry and hot weather for much of the year (Karl and Young 1987). Drought most recently plagued the region between 2006-2009. Bermuda high pressure systems have been linked to soil moisture and drought trends. Variations in the location and strength of the Bermuda High are quantified by the Bermuda High Index (BHI). A positive phase is correlated with strong southerly flow and enhanced precipitation for the eastern U.S. A negative phase is associated with semi-permanent high pressure over the Southeast and consequently drier conditions (Doublin and Grundstein 2008). Fig. 2.1 illustrates the position of the Bermuda High and airflow over the southeastern United States.

There are several types of drought and it is useful to review the most commonly used definitions. Meteorological drought is a regional-specific term that refers to a precipitation departure from normal. The definition varies in both time and space, depending on what is “normal” for a location. Agricultural drought is used when a certain crop or group of crops do not have the sufficient amount of soil moisture needed (Dracup et al. 1980, Wilhite and Glantz 1985). It is measured by the short-term changes to the volumetric soil moisture in the root zone (Keyantash and Dracup 2002). The method includes balancing precipitation and evapotranspiration to determine soil moisture surplus or deficit (Doublin and Grundstein 2008). Because agriculture is an important contributor to the economy, agricultural drought can cause devastating economic losses. Hydrological drought is defined as a decline in subsurface and surface water levels as measured by streamflow and small water bodies such as lakes and reservoirs. In general terms, drought is a deficit in the bulk water supply. Model-reconstructed historical droughts for the U.S. from 1920-2003 showed the most severe agricultural droughts are typically correlated with the most severe hydrological droughts (Andreadis et al. 2005). Socioeconomic drought refers to the point when the water shortage begins to affect communities in terms of supply and demand (Dracup et al. 1980, Wilhite and Glantz 1985). It is measured in monetary terms and is only referred to when one or more of the physical droughts are occurring (Keyantash and Dracup 2002).

Common drought indices used, especially with agricultural and meteorological drought, are Percent Normal, the Palmer Drought Severity Index (PDSI), Palmer *Z*-index, and Standardized Precipitation Index (SPI). Percent Normal compares observed and normal precipitation for a time and location (Quiring 2009). The PDSI measures cumulative moisture departures for homogeneous regions by taking into account precipitation, temperature, and soil water content in a water balance equation. The Palmer *Z*-index is derived from the same data, but is not influenced by the previous month's moisture conditions. The SPI relies on observed rainfall as a standardized departure from a rainfall probability distribution function. Other drought indices used are crop moisture index, surface water supply index, and rainfall deciles (Keyantash and Dracup 2002).

2.2 Atmospheric Conditions Supporting Tornadic Convection

Supercells are the most common storms to produce tornadoes and are characterized by a co-located updraft/downdraft system, bounded weak echo region, rear-flank downdraft, and core mesocyclone circulation (Fig. 2.2). Strong horizontal shear is characterized by the tornadic vortex signature in radar-derived Doppler velocity fields. Tornadoes often occur within a strong vertical velocity gradient near the hook echo and observationally beneath the right or rear of the wall cloud (Lemon and Doswell 1979).

Factors that promote tornadic activity include southwesterly wind shear, dry transients (or intrusion) at the mid-troposphere, moist transients at low levels, and an increase in CAPE (Muñoz and Enfield 2009). Speed wind shear indicates that the magnitude of winds increase from the surface to higher altitudes creating horizontal vorticity. Directional wind shear, a vertical change in wind direction, contributes to thunderstorm rotation and temperature advection. The combination of speed and directional shear components is referred to as helicity. CAPE is the amount of energy available to accelerate a parcel when conditional instability is released, or positive buoyancy (Williams and Renno 1993). CAPE increases as the difference between the parcel temperature and environmental temperature increases. CAPE values larger than 2500 J kg^{-1} imply the potential for strong convection. CIN refers to the counterpart to CAPE, or the negative buoyancy that suppresses convection.

2.3 Land Surface Effects on Convection

Studies have shown that differential heating caused by wet-dry soil boundaries can initiate a thermal circulation in a conditionally unstable atmosphere (Rabin et al. 1990, Hong et al. 1995). The circulation mixes air in the planetary boundary layer, destabilizing it, which allows convective clouds to develop. If enough moisture is available, the clouds produce rainfall. These wet-dry boundaries can form from previous rainfall, deforestation boundaries, and alternating bare soil-vegetation areas. Other studies have shown that wet soil itself, due to sensible and latent heat fluxes, can transport energy and moisture into the atmosphere to enhance CAPE (Clark and Arritt 1995, Bosilovich and Sun 1998, Lynn et al. 1998). These fluxes create “land-land breezes” that help lift parcels to initiate convection (Hanesiak et al. 2004). Moisture transfer through plant evapotranspiration can also cause differential heating in the atmosphere, leading to local thermal circulations and convective instability (Chang and Wetzel 1990, Pan et al. 1996, Hanesiak et al. 2004, Alonge et al. 2006, Iwasaki et al. 2008, Frye and Mote 2010).

Convective cloud development, particularly shallow cumulus, is affected by temporal and spatial changes in the landscape. Convective rainfall intensity and distribution is especially influenced by soil moisture regimes in a dry atmosphere due to water vapor availability. Accumulated precipitation generally increases with maximum latent heat flux (Rabin et al. 1990; Chen and Avissar 1994). Convective rainfall can be enhanced by increased soil moisture when large scale forcing is weak due to differential heating and thermal circulations. Shading by low cumulus can reduce convective rainfall over moist, bare soil (Clark and Arritt 1995, Gallus and Segal 2000, Trier et al. 2004). In semiarid regions, irrigation and vegetative banding can alter rainfall patterns (Anthes 1983, Lanicci et al. 1987). Wet soil regimes have been shown more favorable in producing convective rainfall than dry-soil regimes (Bosilovich and Sun 1998, Alonge et al. 2006, da Silva and Avissar 2006, Iwasaki et al. 2008). In west Africa, deforestation and desertification result in less rainfall (Zheng and Eltahir 1998) while in deforested regions of the Amazon cloudiness increased but effects on precipitation are negligible (da Silva and Avissar 2006).

Dry soil by itself ultimately reduces the amount of rainfall that could be produced if storms do develop. Dry soil allows the planetary boundary layer (PBL) to grow to greater depths, which reduces thermodynamic instability, whereas wet soils produce a moist, shallow PBL with higher CAPE (Lanicci et al. 1987, Segal et al. 1995, Alonge et al. 2006). The PBL is the lowest layer of the atmosphere directly affected by the surface of the earth, including soil moisture, and ranges anywhere from 30 m if very stable to 3 km in convectively unstable conditions. Wind velocity essentially disappears at the surface, causing large velocity shear and turbulent eddies. Shear-induced eddies and convective eddies from surface heating effectively transfer momentum to the surface and heat upward. The main source of boundary layer turbulence depends on the structure of the wind and temperature profiles near the surface. An unstable lapse rate is associated with convectively generated turbulence, while a stable lapse rate is associated with wind shear-generated turbulence (Holton 2004). The boundary layer has a distinct diurnal evolution. At night, longwave radiation freely leaves the surface (especially under clear skies), dropping the temperature, and causing a stable surface layer or inversion. This suppresses vertical motion and turbulence. After sunrise, the surface absorbs solar radiation which increases positive buoyancy, eliminates the nocturnal inversion, and enables the convective layer to advance upward (Salby 1996).

The evolution of the PBL during the course of a day can be seen in Fig. 2.3. Fig. 2.4 shows plots of domain-averaged CAPE for wet and dry soil moisture regimes in the Sahel on a day of convective activity. The higher CAPE in the wet regime is attributed to a slow-growing PBL less prone to entrainment of drier air aloft (Alonge et al. 2006). However, Frye and Mote (2010) found that CAPE is high and CIN is low over dry soils in the southern Great Plains during the warm season. The relationship between CAPE and soil moisture is dependent on the synoptic scale patterns present. Wet soils have lower sensible heat flux because energy is first used to evaporate surface water. The higher sensible heat flux over dry soils increases the temperature, causing upward motion and convergence. Frye and Mote (2010) suggested that more severe convection is likely on days with a low-level jet (LLJ) and wet soils. On days with no LLJ, CAPE decreases with increasing soil moisture and thunderstorm development is likely to be more severe over dry soils. Dryline strength and movement have been shown to be sensitive to soil moisture distributions in the Southern Plains through changes in the elevated mixed layer and displacement of low-level convergence (Lanicci et al. 1987).

2.4 Soil Moisture Memory

Some studies have shown that soil moisture conditions create "soil moisture memory" that affects future convective activity (Pal and Eltahir 2001, Wu and Dickinson 2004). Due to the large heat capacity of the ocean, anomalies in ocean characteristics change slowly. Similarly, land surface anomalies change slowly relative to the atmosphere, but are not well understood (Dirmeyer et al. 2008). Meng (2009) points out that until recently, there were a lack of soil moisture observations to adequately study soil moisture persistence.

Meng (2009) suggests the importance of soil moisture memory is dependent on the climatic region, soil depth, and vegetation type of the area. Douville et al. (2007) indicate that soil moisture memory increases with latitude and is controlled by the seasonality of the atmosphere, evaporation, variation of runoff with soil moisture, and coupling between land and atmosphere. Areas in the U.S., among other "hotspots" such as western Africa, have been named as regions where soil moisture and precipitation are strongly linked (Kim and Wang 2007). Specifically, Jiang et al. (2009) conclude that strong coupling exists in the central U.S. in the transition zone between wet and dry regions. It has been found that soil moisture memory in tropical climates lasts longer in dry conditions and deeper soils. Kim and Wang (2007) found that in the U.S. dry anomalies in deep soils last months longer than those in shallow soils. Under wet conditions, soil moisture memory is likely controlled by the climate while under dry conditions soil moisture relies on evapotranspiration and runoff (Wu and Dickinson 2004). It should be noted that none of these studies address convective hazards, such as tornadoes, but focused on precipitation.

Observations and model simulations indicate that the timescale of soil moisture variability is 2-3 months in the midlatitudes and can therefore impact precipitation on a seasonal scale (Wu et al. 2007, Dirmeyer et al. 2008). Numerical experiments revealed that soil moisture-rainfall feedback plays an important role in sustaining drought conditions or flood conditions (Pal and Eltahir 2001). Climate models that do not correctly represent soil moisture memory may underestimate precipitation, particularly in dry regions (Wu et al. 2007). Soil moisture persistence and its role in land-atmosphere interaction are essential to advance water cycle prediction (Dirmeyer et al. 2008). Jiang et al. (2009) also show that consideration of vegetation growth and groundwater dynamics improve summer rainfall simulations.

Drought is common in the Southeast and has many definitions in the literature. For this research, agricultural drought is the closest definition to what will be utilized as it is based on soil moisture available for crops. Soil moisture interacts with the lowest layer of the atmosphere to help initiate convection. Moisture and heat fluxes from soil may provide key ingredients for tornado development in the Southeast, and likewise the lack of these fluxes during drought may hinder tornadic environments. Soil moisture memory may the physical mechanism linking fall/winter soil moisture conditions to the spring tornado season.

Fig. 2.1. Illustration of the strong southerly flow over the study area associated with a Bermuda High over the Atlantic Ocean. This is a positive BHI phase (mean sea level pressure is anomalously high over Bermuda) and brings more precipitation to the southeastern United States.

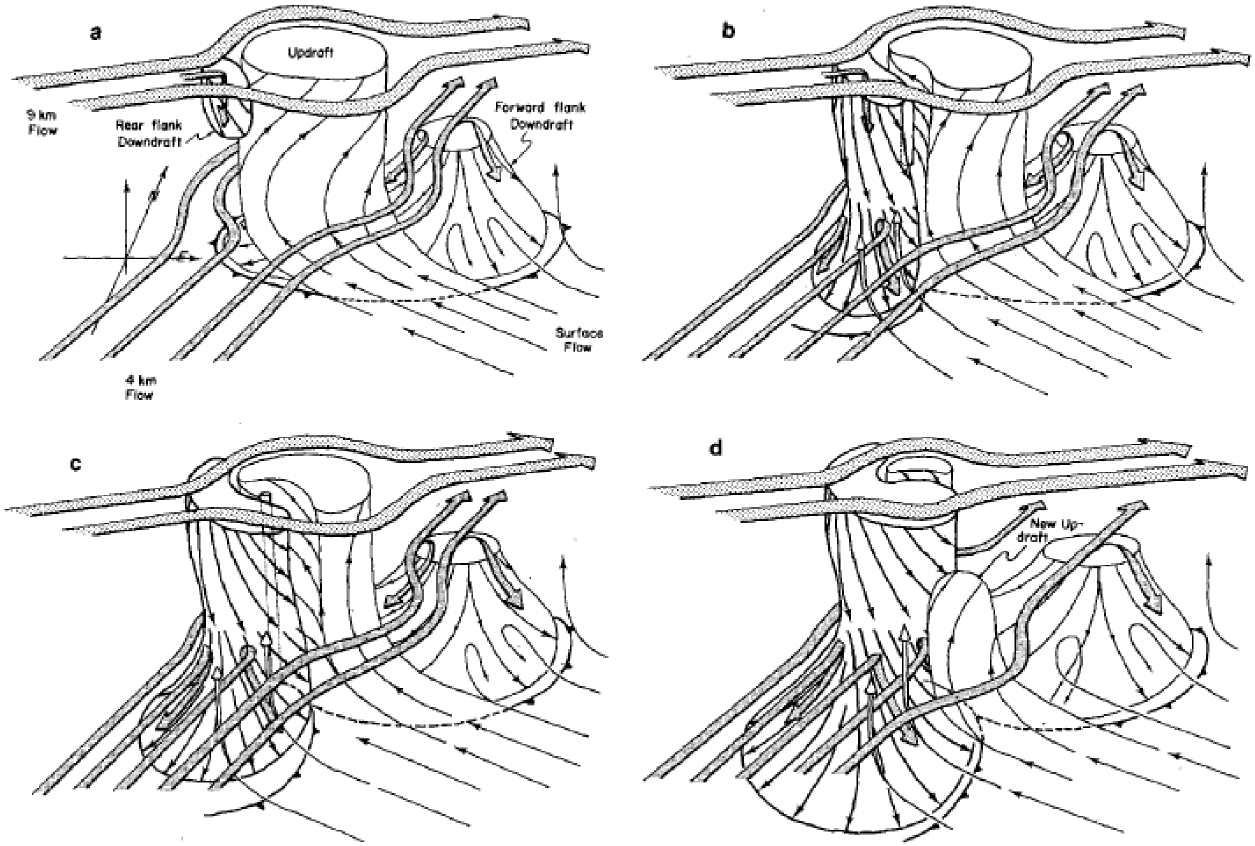

Fig. 2.2. Schematic drawing of the evolution of a supercell storm characterized by a co-located updraft/downdraft system, bounded weak echo region, rear-flank downdraft, and core circulation (from Lemon and Doswell 1979).

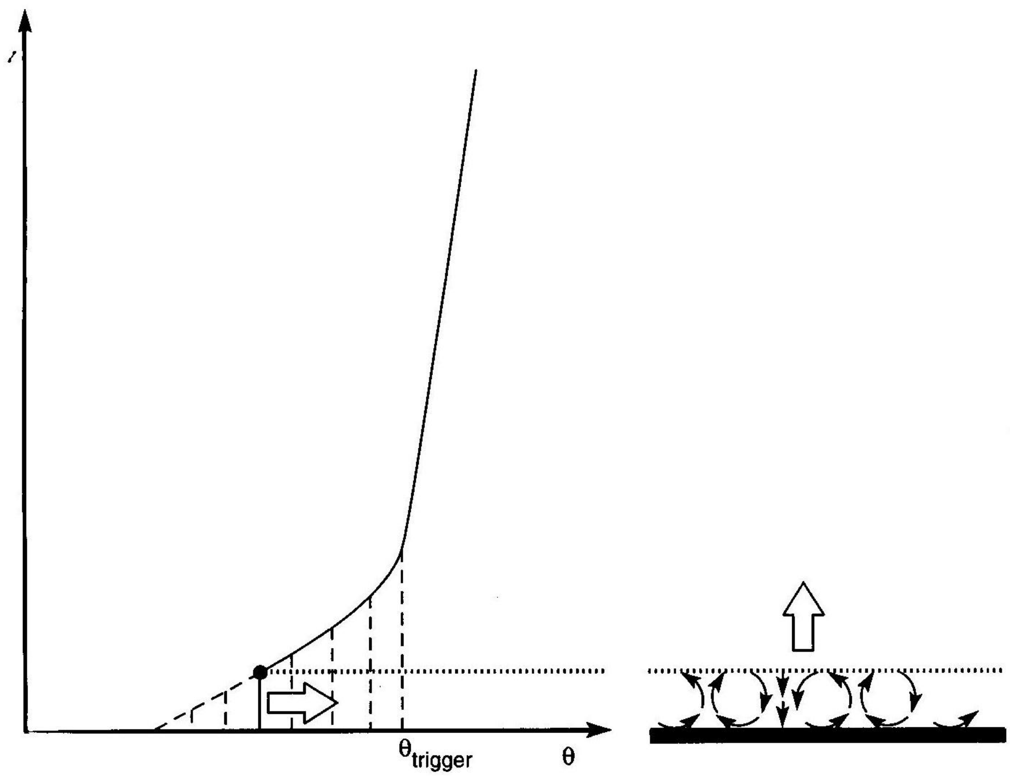

Fig. 2.3. Evolution of the boundary layer (θ is potential temperature). Nighttime cooling causes a shallow, stable layer (nocturnal inversion). After sunrise, the surface temperature increases from absorption of solar radiation. Eventually the trigger temperature is reached and convective turbulence increases rapidly. Turbulence and positive buoyancy near the surface transports heat and momentum upward (from Salby 1996).

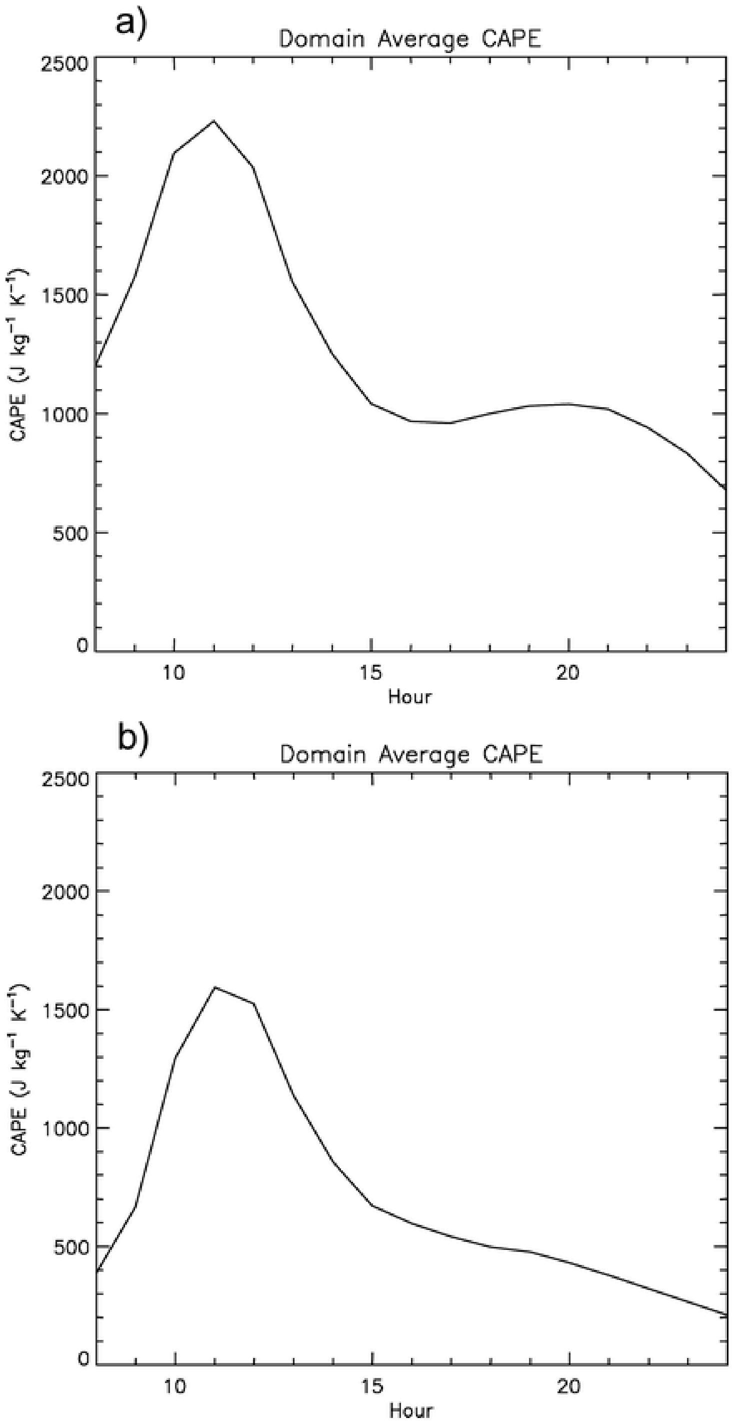

Fig. 2.4. Domain-averaged CAPE time series for (a) wet regime and (b) dry regime (from Alonge et al. 2006).

CHAPTER 3

RESEARCH DESIGN AND METHODOLOGY

3.1 Study Area and Period

This research uses an observational approach to carry out the primary objectives. The southeastern United States study area is defined here as 32°N - 35°N and 82°W - 88°W (Fig. 3.1). The area is chosen to include a representative portion of the Southeast and to exclude the southern-most parts of Georgia and Alabama that might experience coastal convection and associated landspout tornadoes. The southeastern United States is chosen in particular because of the occurrence of droughts and potential to examine drought-convection processes. The time period for this study spans 1980-2006 because of available data and reliability of the tornado reports as compared to pre-1980 records. Past tornado reporting was unreliable and accuracy in the records is limited. Tornado reporting relies on local documentation and inherently has issues related to discontinuities, changes in reporting style, population changes, storm spotter networking, and new technology (Doswell and Burgess 1987, Grazulis 1993, Ashley 2007).

Fig. 3.2 shows all documented tornado occurrences 1980-2006 over the U.S. The southeastern United States has experienced many tornadoes over the 27-year period along with the central and eastern regions of the country. Fig. 3.3 is a map of all tornado occurrences 1980-2006 over the study area. These tornado maps support recent work by Frates (2010) who is calling the swath of tornadoes occurring in the Southeast “Dixie Alley”. The U.S. Drought Monitor has been keeping drought severity records for the past decade. A time series (2000-2010) of the percent area of the southeastern United States within drought conditions is shown in Fig. 3.4. In the last decade, three distinct droughts occurred, two of which left approximately half of the Southeast in extreme drought. It is apparent that the southeastern U. S.

experiences a wide range of soil moisture conditions and both dry and wet soil regimes are useful to this study.

3.2 Tornado and PDSI Data

3.2.1 *Tornado Database*

Tornado data are obtained from the National Oceanic and Atmospheric Administration (NOAA) Storm Prediction Center's (SPC) historical database of severe thunderstorm and tornado occurrences from 1980 to 2006 and analyzed with SeverePlot V2 graphical tool (http://www.spc.noaa.gov/software/svrplot2/). The Enhanced Fujita-Scale (EF-Scale) was not implemented until 2007, therefore all tornadoes are reported as F-Scale for this research. The F-Scale categorizes tornado damage based on wind speed ranging from F0 (light damage) to F5 (incredible damage). A monthly count of F0-F5 tornadoes for the study area (1980-2006) reveals F3+ tornadoes are most frequent during March (Table 3.1).

March, April, and May are best defined as the tornado season (Fig. 3.5) as they have totals more than twice the preceding (February) and following (June) months. For the purposes of this study, antecedent periods are based on the tornado season. Therefore, February is the 1-month antecedent period, January and February comprise the 2-month antecedent period, and September through February comprise the 6-month antecedent period. These antecedent periods are used instead of individual months in order to capture any short-term and long-term drought periods that occurred.

The number of tornado days and number of multiple tornado days per season are also calculated. A tornado day is any day during the tornado season that experienced a tornado. A multiple tornado day is any day during the tornado season that experienced more than one tornado. The number of tornado days averages about 5 per season (Fig. 3.6). A histogram shows tornado days are right (positively) skewed (Fig. 3.7) meaning high counts of tornado days are less frequent than low counts. The number of multiple tornado days averages about 2.8 per season (Fig. 3.8). A histogram shows multiple tornado days are slightly right skewed (Fig. 3.9). More robust statistical analysis is required to quantify temporal and spatial trends.

3.2.2 *PDSI Z-Index*

Monthly PDSI *Z*-index values are the measure of the departure from normal of the moisture climate for a climate division or state during a month. The *Z*-index reflects short term soil moisture conditions. Monthly values for six climate divisions are obtained for the study period from the National Climatic Data Center (NCDC) at http://www1.ncdc.noaa.gov/pub/data/cirs/. Six divisions were used in order to cover an adequate sample of the study area. The values are averaged to obtain 1-, 2-, and 6-month means for each year. The index classifies drought as any *Z* value equal to or below -1.25 standard deviations, but the data are analyzed for an appropriate threshold that may be above or below the operational definition. The PDSI *Z*-index is utilized in this research only for the purpose of assessing how well normalized soil moisture data from NARR captures drought and for choosing the correct threshold. For all following analyses, a period is defined as drought based on the NARR soil moisture threshold.

3.3 NARR Data

This study utilizes data from the North American Regional Reanalysis model (NARR). NARR uses the high resolution (32km/45 layer) NCEP Eta model in conjunction with the Regional Data Assimilation System. It is run eight times per day and incorporates the Noah Land-Surface Model (Fig. 3.10). The data are available for download from NOAA Earth System Research Laboratory (ESRL) Physical Sciences Division (PSD) at http://www.cdc.noaa.gov/cgi-bin/data/narr/plotmonth.pl. The website contains a monthly/seasonal climate composite tool that outputs the data onto a 349 x 277 Lambert Conformal Conic grid. Fig. 3.11 illustrates the coverage area for sample data. The variable, season, years, and contour interval can be selected for a customized projection. Both the image and the corresponding data file are generated with the composite tool. The data file is outputted as a network Common Data Form (netCDF), which stores the gridded data as an array (NARR 2010). An analysis tool called *Ferret* (http://ferret.wrc.noaa.gov/Ferret/) is used to locate values for the specified latitudes and longitudes and output the data into an ASCII file. The study area coordinates most closely correspond to gridpoints i = 229:249, j = 88:103 in the NARR grid. Although daily values are used for the monthly means, future studies might consider the 0z data alone, which might better represent the most convectively active time of the day. The following sections describe the NARR variables utilized.

3.3.1 *Soil Moisture*

NARR contains four soil layers (0-10, 10-40, 40-100, 100-200 cm), with three prognostic soil states available for each layer. Total soil moisture (sum of liquid plus frozen moisture) is utilized here. Monthly mean soil moisture is obtained for the specified gridpoints at 1-, 2-, and 6-month antecedent periods to the spring season and also spring of each year. The soil moisture content variable is valid at the midpoint of the 0-100 cm soil layer for monthly means and is reported as a volumetric fraction ($kg \cdot m^{-2}$). Soil moisture content, as opposed to precipitation data or PDSI, is selected because future satellite (SMAP mission, http://smap.jpl.nasa.gov/), in-situ, and reanalysis datasets (NARR, MERRA-http://gmao.gsfc.nasa.gov/research/merra/intro.php) will provide similar spatio-temporal measurements, which facilitates a more meaningful comparison. However, future research might consider repeating this methodology with more traditional drought indicators as well.

3.3.2 *Convective Parameters*

Monthly mean CAPE ($J \cdot kg^{-1}$) and CIN ($J \cdot kg^{-1}$) values at the surface for February are analyzed with composite maps and statistically in Excel. Surface parcel CAPE, also called SBCAPE, uses surface temperature and dew point to determine parcel lift and buoyancy. SBCAPE is a better measure of surface-based convection and the potential for tornadoes than lower atmosphere CAPE (MUCAPE) and may link surface-atmosphere interactions (Bunkers et al. 2002). However, recent work has shown that NARR MUCAPE may be preferable as it is less sensitive to data spikes and may represent both surface-based and elevated conditions (Bunkers et al. 2009). SBCAPE and MUCAPE are often comparable in the afternoon to early evening when the surface parcel is at maximum instability. Future work may evaluate the merits of both measures, but it is beyond the scope of this study. Additionally, further research may utilize 3-hourly composites, rather than daily, to avoid averaging inactive CAPE periods. Only CAPE and CIN values for the 1-month antecedent period are analyzed as values prior to February may not be linked to the spring season. These variables best represent the stability of the atmosphere from the available parameters NARR offers. Mathematically CAPE is represented as:

$$CAPE = R_d \int_{EL}^{LFC} (T_v{'} - T_v)(d \ln p) \quad \textbf{(Eq. 1)}$$

where R_d is the gas constant for 1 kg of dry air, *EL* is the equilibrium level, *LFC* is the level of free convection, $T_v{'}$ is the parcel's virtual temperature, and T_v is the environmental virtual temperature. *Virtual temperature* is the temperature dry air would need to reach in order to attain the same density as moist air at the same level (Wallace and Hobbs 2006). CAPE and CIN are adequate measures of instability, but future studies may also utilize shear and helicity parameters for insight into rotation available for tornadoes.

3.3.3 *Geopotential Heights*

Monthly mean 500 hPa geopotential height composite maps are used to assess the synoptic environment prior to the tornado season, during drought and non-drought conditions. The National Weather Service describes "synoptic scale" as weather patterns ranging from 1,000 km to 2,500 km wide. Five-hundred hPa heights reveal general trough and ridge patterns, high and low pressure systems, and indirectly show the position of the jet stream (direct analysis would utilize 200-300 hPa levels). Areas of ridging are associated with higher pressure and warmer temperatures relative to troughs which are associated with lower pressure and cooler temperatures. Fig. 3.12 illustrates a generalized synoptic scale trough and ridge pattern. Severe weather is often associated with troughs because air converges at the low pressure center at the surface and is forced upward. Rising air cools and condenses to form clouds. If the atmosphere is sufficiently unstable, then storms may develop. Similarly, rising air and severe weather often occur along a frontal boundary (the boundary of two dissimilar air masses). Temperature advection due to circulation around pressure systems, jet streams, and positive vorticity advection can also help initiate vertical air movement. If no major synoptic scale features are present, then convection might be attributed to forcing at the surface.

3.3.4 *Mean Sea-Level Pressure*

Monthly mean sea-level pressure (MSLP) in units of Pascals (Pa) are obtained for

- Bermuda (32.33°N, 64.75°W) and area-averaged over the 1-month antecedent period, the 6-month antecedent period, and the warm season (May-September) and
- The southeastern United States and area-averaged over the 1-month antecedent and the 6-month antecedent periods.

The values for the two locations are used to calculate a modified BHI for the warm season and antecedent periods. The BHI is an index of the pressure change across the Atlantic may influence precipitation and drought conditions across the Southeast.

3.4 Research Methodology

3.4.1 *Statistics*

The strength of the relationship between datasets is quantified with Pearson's correlation coefficient (*R*). The coefficient is a standardized convariance, or numerical measure of the degree to which two variables shift within statistical space. It is mathematically represented as:

$$R_{(x,y)} = \frac{s_{xy}}{s_x * s_y} \qquad \textbf{(Eq. 2)}$$

where s_{xy} is the covariance, s_x is the variance of variable *x*, and s_y is the variance of variable *y*. An *R* value of -1.0 is the maximum negative correlation. Values ranging from 0.0 to -0.33 indicate a weak relationship, 0.33 to 0.66 a moderate relationship, and 0.66 to 1.0 a strong relationship. A smaller coefficient indicates there is greater dispersion from the line of best fit. *R* defines the direction and strength of the relationship, but does not describe the magnitude.

The statistical significance of the correlation is quantified using a T-Test. This employs the null hypothesis that there is no correlation between the two variables (R = 0). The alternative hypothesis is that there is a significant positive correlation between the two variables ($R > 0$). Using the table for t-distribution critical values, the significant level of R is found for a one-tailed test at the 95% confident level ($\alpha = .05$). The T-Test is performed and a decision is made to accept or reject the null hypothesis. The correlation between the variables can then be characterized.

3.4.2 *Drought Periods*

Drought periods are calculated from the soil moisture content data using a modified *z*-score. Although the current *normal period* is defined between 1970-2000, the NARR data are not available until 1979 so years 1980-2006 are used to normalize the data. First, the boundaries for the first three climate divisions in each state are approximated by matching the NARR grid coordinates to the latitude and longitude along the division borders. All of the NARR grid points within each zone are noted. The average (x) and standard deviation (σ) of the soil moisture values lying within Alabama Climate Zone 1 for each antecedent period are calculated, and the average (μ) over all of the years (for the respective antecedent period) is calculated in order to find the *z*-score:

$$z = \frac{x-\mu}{\sigma} \qquad \textbf{(Eq. 3)}$$

The calculations are repeated for Alabama climate divisions 2 and 3, and Georgia climate divisions 1-3, for all antecedent periods. Once a *z*-score is assigned to each division-averaged period, a logical test (e.g. an IF-THEN statement) is performed to identify which periods had *z*-scores below -0.75 standard deviations and below -1.0 standard deviations, similar to Doublin and Grundstein (2008). Both standard deviations are used to determine the correct threshold for categorizing drought conditions by comparing them to the Palmer *Z*-index drought periods. Based on the six climate zones, it is determined that normalized soil moisture values below -1.0 indicate drought periods most appropriately and are used as the drought threshold. Table 3.2 shows the 6-month analysis for Alabama Climate Zone 1 as an example.

3.4.3 *Tornado Days*

To analyze drought periods in relation to tornado days, the soil moisture values are averaged over the study area for each 6-month period, and a *z*-score is calculated for each period. The percent of normal tornado days is found by averaging the tornado days (per season) over the 27-year period, then dividing each seasonal value by the total average and multiplying by 100%. The soil moisture departures are correlated with percent of normal tornado days using linear regression analysis and tested for significance with a T-Test.

3.4.4 *Tornado Track Distributions*

ArcMap GIS is used to examine the spatial occurrence of tornadoes during tornado seasons following drought years and non-drought years, respectively. Rank analysis is done to sort the years by lowest to highest soil moisture departures. This allows the six drought years and six wettest years to be identified and used for the analysis, eliminating the bias of the unequal number of drought to non-drought years (Table 3.3). For the remainder of this thesis, the term "drought years" refers to the six drought years and "non-drought years" refers to the six highest soil moisture years, unless otherwise stated.

To digitize the tornado tracks maps to make a composite, projected base maps of the two states in the study area, Alabama and Georgia, were used. The states' shapefiles are taken from the NOAA National Geodetic Survey website (http://www.ngs.noaa.gov/cgi-bin/sf_archive.prl). The horizontal datum is The North American Datum of 1983 with units in degrees, minutes, and decimal seconds (DMS). Two personal geodatabases were created, one for each map, each with a "line" feature class to represent the tornado tracks. The feature classes were set to the same coordinate system as the state shapefiles.

The tornado maps are added to the ArcGIS session as bitmap images. The SeverePlot program displays coordinates in decimal degrees, so the four corners of the maps are noted and converted to DMS. The "drought" tornado maps are individually georeferenced to the state shapefiles by inputting the DMS points at the four corners. Once georeferenced, the map is digitized using the "editing" function of ArcMap. By hand, the tracks are selected and saved to the feature class. This procedure is repeated for all of the drought maps and edits are saved to the same feature class, creating a composite of all tornado occurrences for all drought years. The georeferencing and digitizing is repeated for tornado track maps during antecedent non-drought years (six wettest).

3.4.5 *Convective Parameters & Synoptic Conditions*

The relationship between soil moisture and atmospheric instability is investigated using the convective parameters CAPE and CIN. The monthly mean CAPE and CIN values are composited for drought and non-drought years, respectively, and also area-averaged for correlation analysis. Scatterplots and time series plots are used to analyze the convective parameter in relation to soil moisture. Pearson's correlation analysis is employed and a T-Test is used to test the significance of the correlation coefficient. The synoptic environment is examined by compositing 500 hPa geopotential heights across the domain for drought and non-drought regimes.

3.4.6 *Soil Moisture Memory*

Soil moisture memory is evaluated from fall/winter to spring of the next year by using time series correlations and scatterplots. The soil moisture values are normalized using the *z*-score method. Fall/winter soil moisture is investigated for any tendencies to persist into the spring season. The intent is to create a predictor equation or table that could describe the tornado season intensity based on fall/winter soil moisture conditions.

3.4.7 *BHI*

Similar to Doublin and Grundstein (2008), the BHI is calculated by subtracting the standardized monthly sea-level pressure for the study area from the Bermuda standardized sea-level pressure. This is a modified version of the BHI as it is usually defined as the pressure difference between Bermuda and New Orleans. The data are standardized using the same methodology as soil moisture by area-averaging the data for each time period, then calculating the *z*-score for each. The positive and negative phases of BHI are correlated to the drought periods using Pearson's product-moment correlation. Although Doublin and Grundstein (2008) correlated warm season BHI with soil moisture, it is the intent of this study to see if fall/winter BHI is also related to concurrent soil moisture conditions.

In summary, Palmer *Z*-index data are used to help set up a threshold for soil moisture-indicated drought by correlating *Z*-index and soil moisture *z*-scores within six climate divisions. NARR data and tornado data for the 27-year period are utilized to examine the potential relationship between drought and tornado occurrences. The NARR data are area-averaged over the entire Southeast study area and analyzed with composite maps, scatterplots, and time series graphs. Pearson's product-moment correlation and the T-Test are used to quantify the significance of results.

Table 3.1. Monthly count of Fujita categorized tornadoes in the southeastern United States, 1980-2006.

Category	Jan	Feb	Mar	April	May	June	July	Aug	Sept	Oct	Nov	Dec
F0-F5	39	60	130	161	137	56	48	59	64	17	137	33
F0	14	12	42	55	49	24	31	22	35	6	39	14
F1	15	33	59	71	68	24	16	26	21	7	51	11
F2	8	11	14	27	17	7	1	10	8	4	37	4
F3	2	4	13	7	2	1	0	1	0	0	6	3
F4	0	0	2	0	1	0	0	0	0	0	4	1
F5	0	0	0	1	0	0	0	0	0	0	0	0

Table 3.2. Six-month drought analysis for Alabama climate division 1.

Alabama Division 1		
	Z-INDEX	SOILM
1980, 6-MO	0.41	1.61
1981, 6-MO	-0.59	-1.07
1982, 6-MO	0.19	-0.88
1983, 6-MO	-0.16	0.28
1984, 6-MO	0.17	0.35
1985, 6-MO	-0.09	0.38
1986, 6-MO	-0.92	0.09
1987, 6-MO	1.22	-0.19
1988, 6-MO	-0.39	-1.20
1989, 6-MO	1.49	-0.90
1990, 6-MO	1.23	1.98
1991, 6-MO	1.30	-0.36
1992, 6-MO	-0.29	0.61
1993, 6-MO	0.20	0.59
1994, 6-MO	0.87	-0.19
1995, 6-MO	0.18	0.59
1996, 6-MO	0.78	0.22
1997, 6-MO	0.95	0.59
1998, 6-MO	1.28	0.95
1999, 6-MO	-0.31	-0.65
2000, 6-MO	-1.33	-2.33
2001, 6-MO	-0.45	-1.99
2002, 6-MO	0.25	0.24
2003, 6-MO	0.58	0.63
2004, 6-MO	0.14	0.47
2005, 6-MO	0.99	1.06
2006, 6-MO	-0.64	-0.88

Table 3.3. Soil moisture departures for drought and non-drought years.

Drought Years		Non-Drought Years	
2001	-1.82	1990	1.70
2000	-1.61	1995	1.53
1988	-1.29	1993	1.35
1982	-1.19	1998	1.16
1989	-1.11	1980	1.08
1981	-1.11	2004	1.07

Fig. 3.1. Southeastern United States study area encompassing northern Georgia and northern Alabama (from Google 2009).

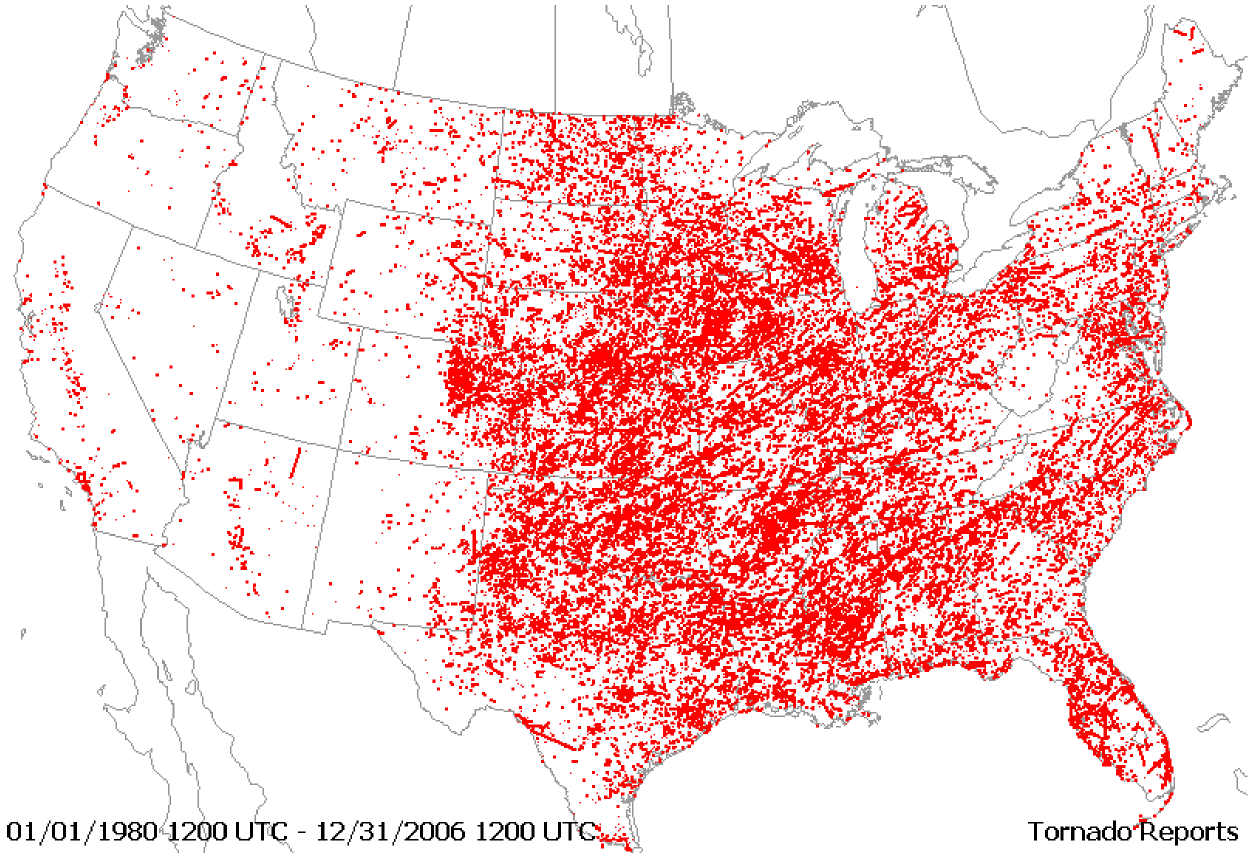

Fig. 3.2. SeverePlot map of all documented tornadoes that occurred 1980-2006 in the United States.

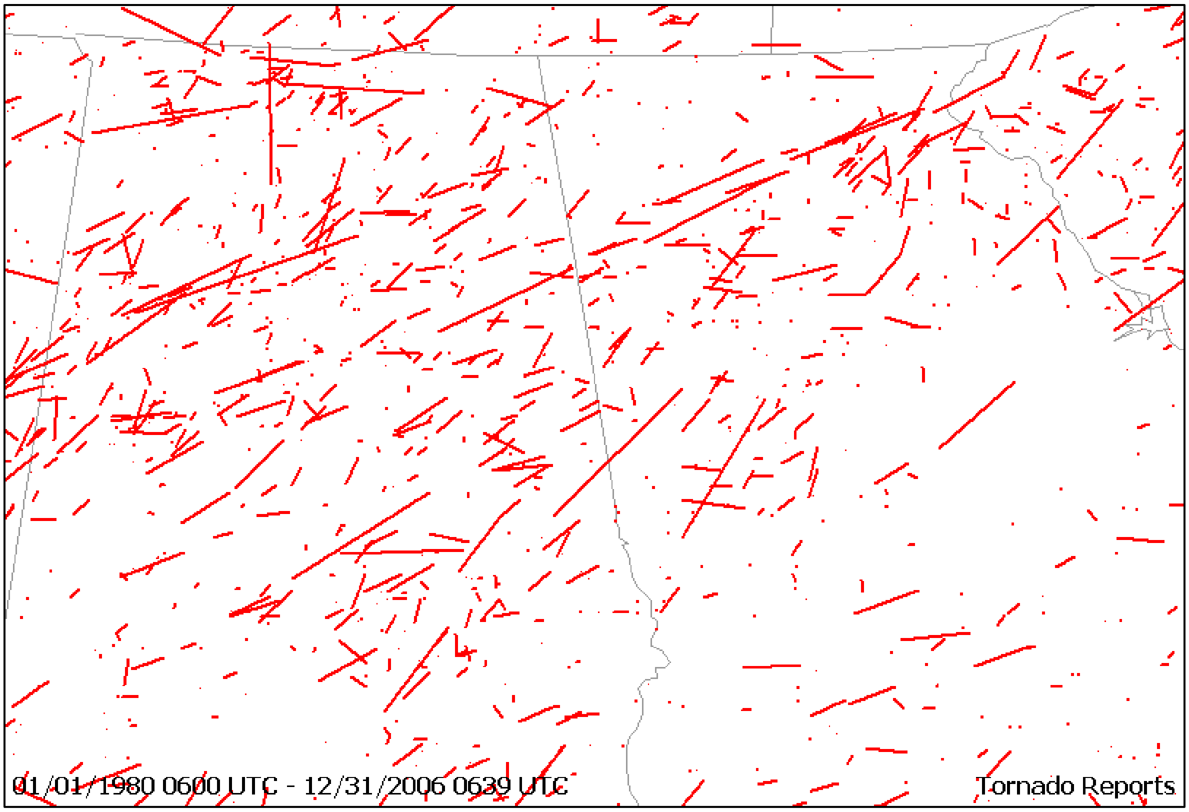

Fig. 3.3. SeverePlot map of all tornado occurrences 1980-2006 for the southeastern United States.

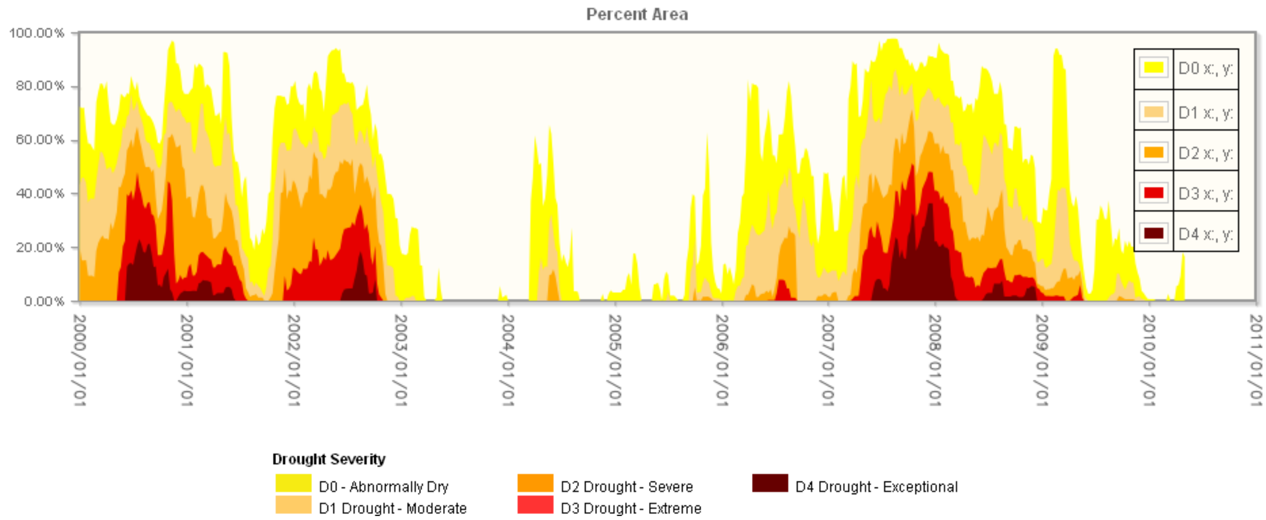

Fig. 3.4. U.S. Drought Monitor time series plot of percent area of the southeastern United States within drought, ranging from abnormally dry to exceptional drought.

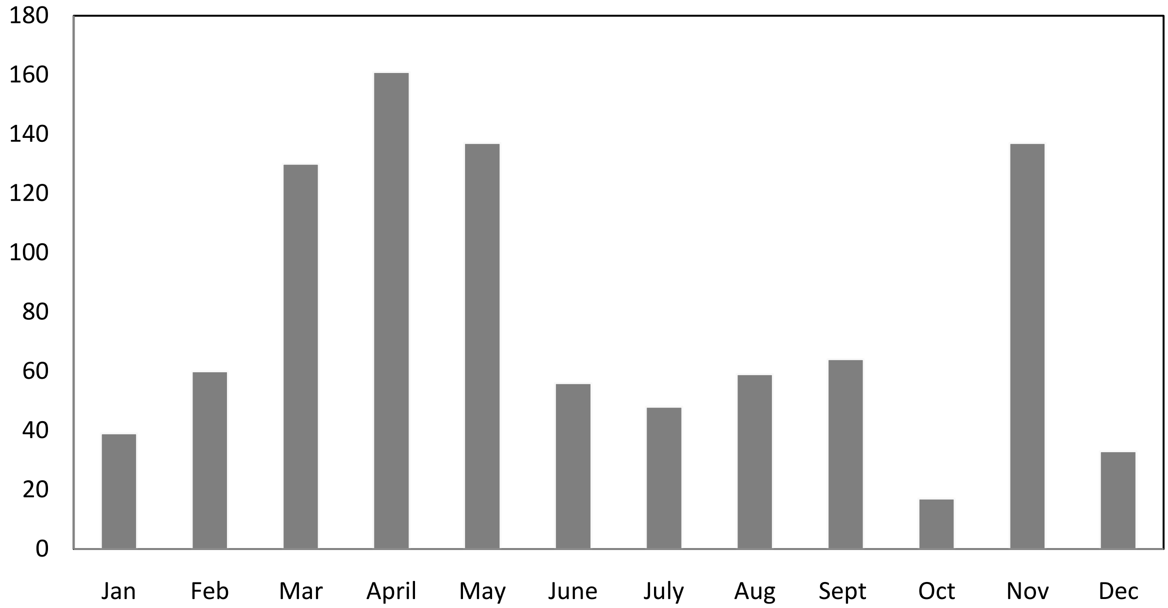

Fig. 3.5. Total tornado occurrence by month for the study area.

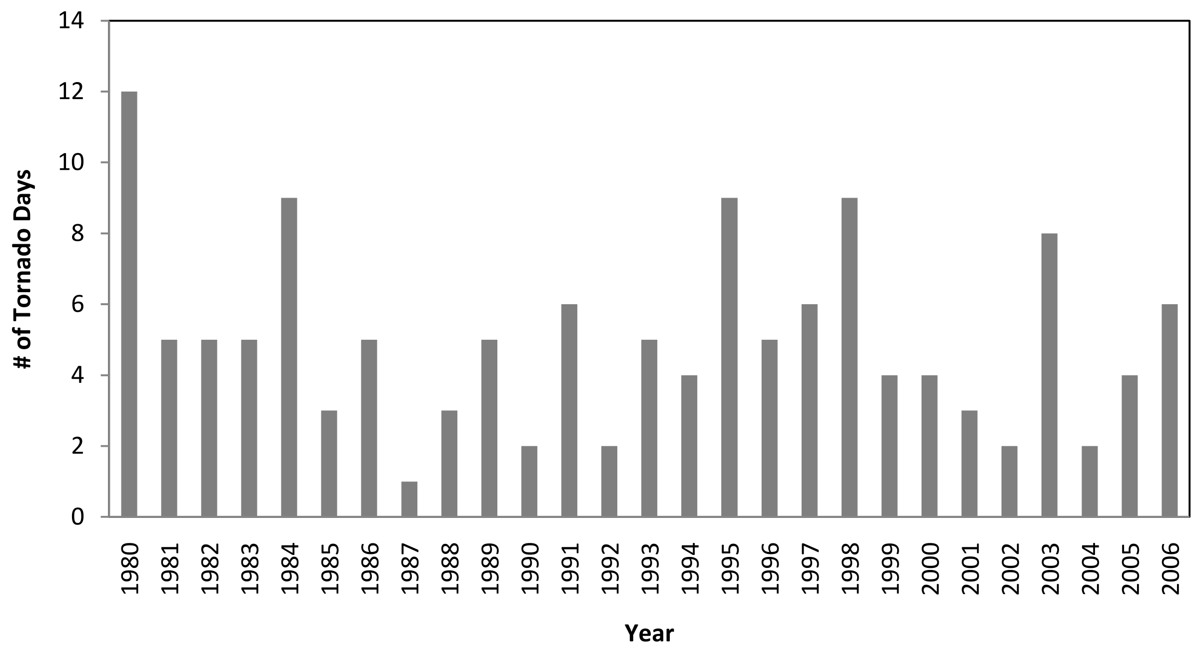

Fig. 3.6. The number of tornado days per tornado season, 1980-2006 (average about 5 per season).

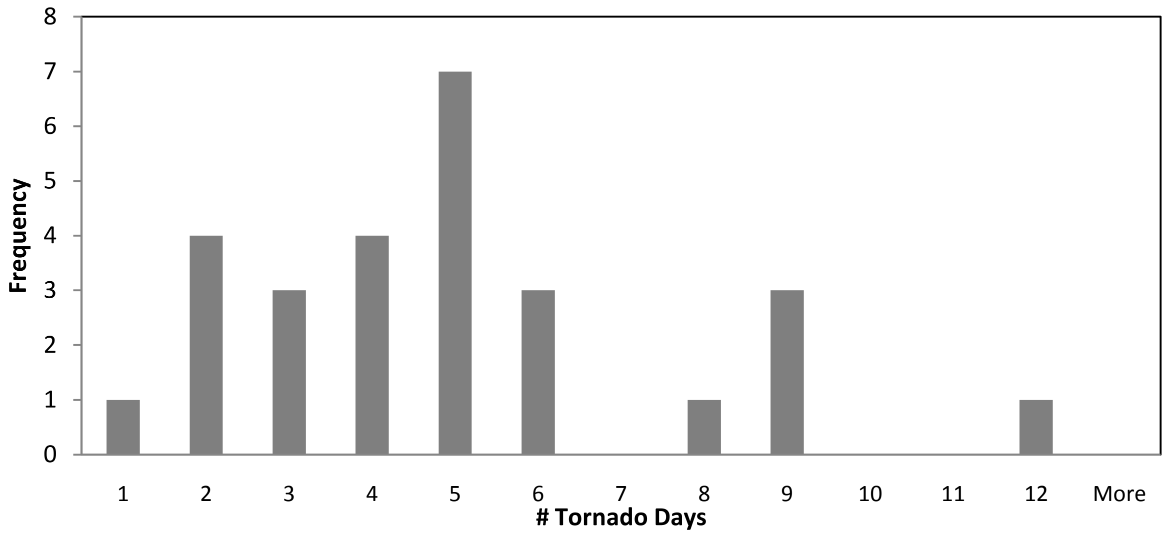

Fig. 3.7. Histogram of the number of tornado days during tornado seasons. Tornado days are right (positively) skewed meaning high counts of tornado days are less frequent than low counts.

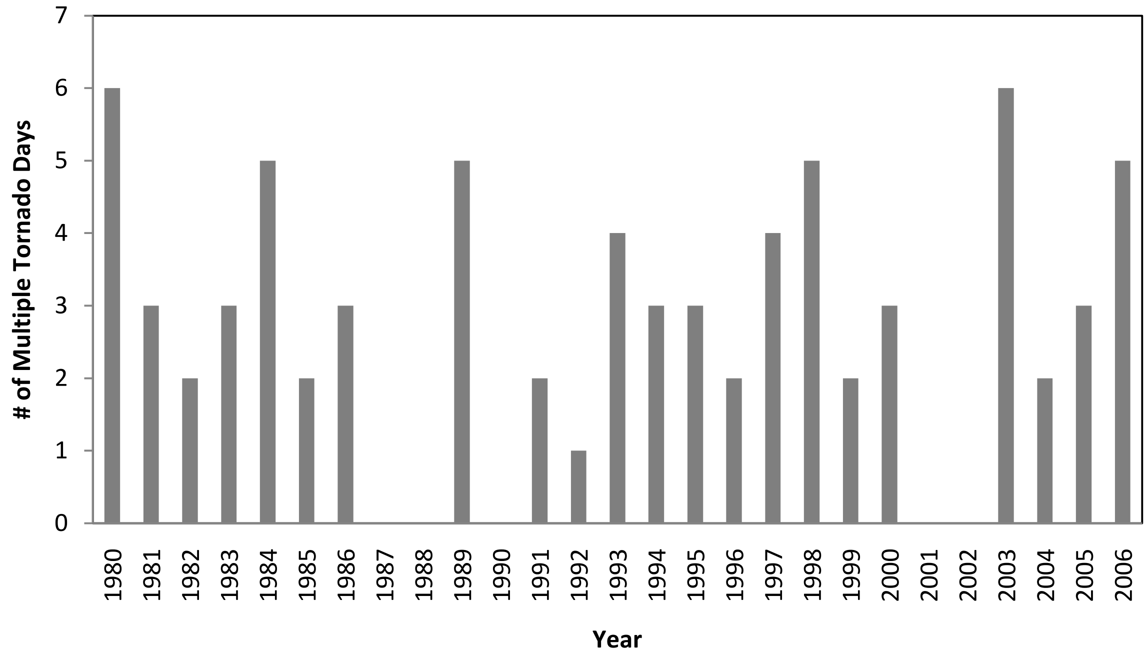

Fig. 3.8. Number of multiple tornado days per season, 1980-2006 (averages about 2.8 per tornado season).

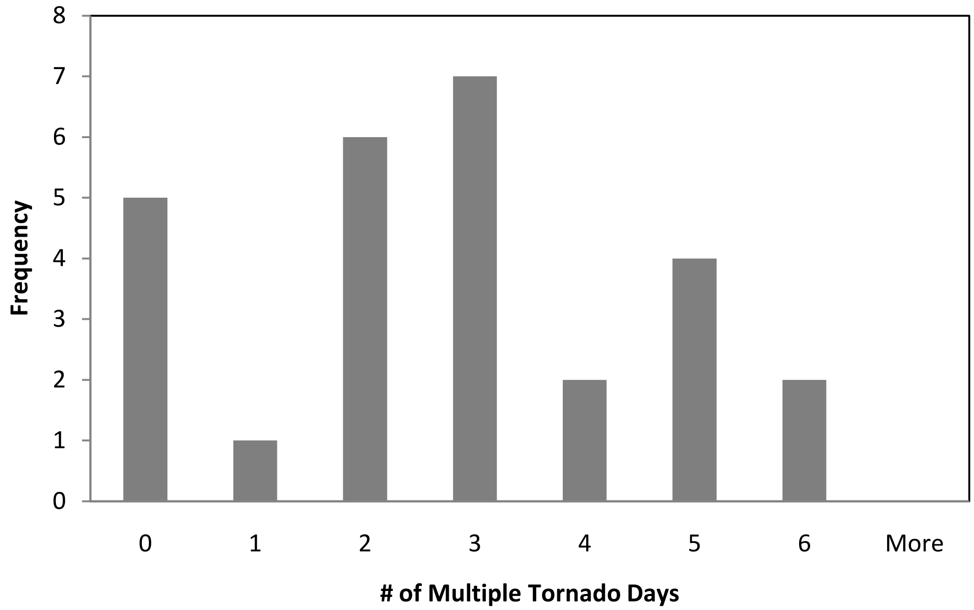

Fig. 3.9. Histogram of the number of multiple tornado days during tornado seasons. Multiple tornado days are slightly right skewed.

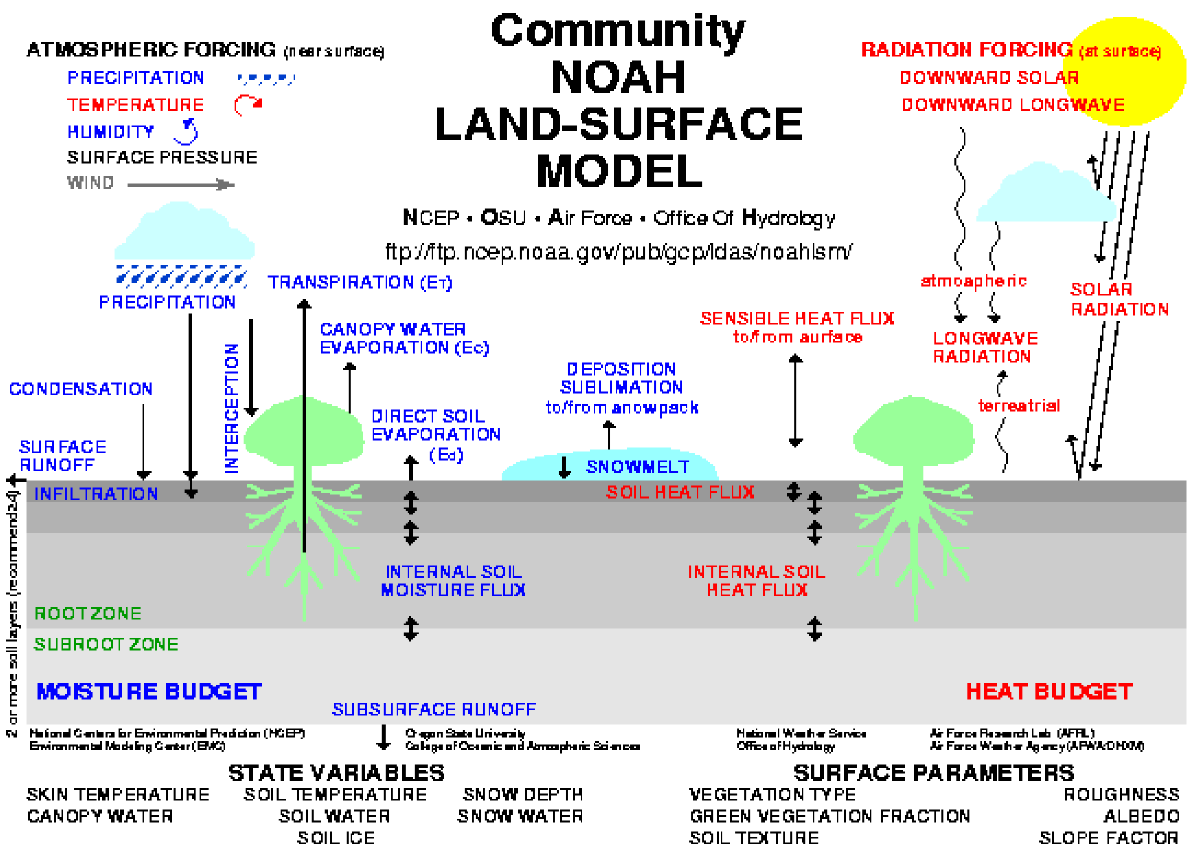

Fig. 3.10. A schematic of the Noah Land-Surface Model in NARR.

(a)

(b)

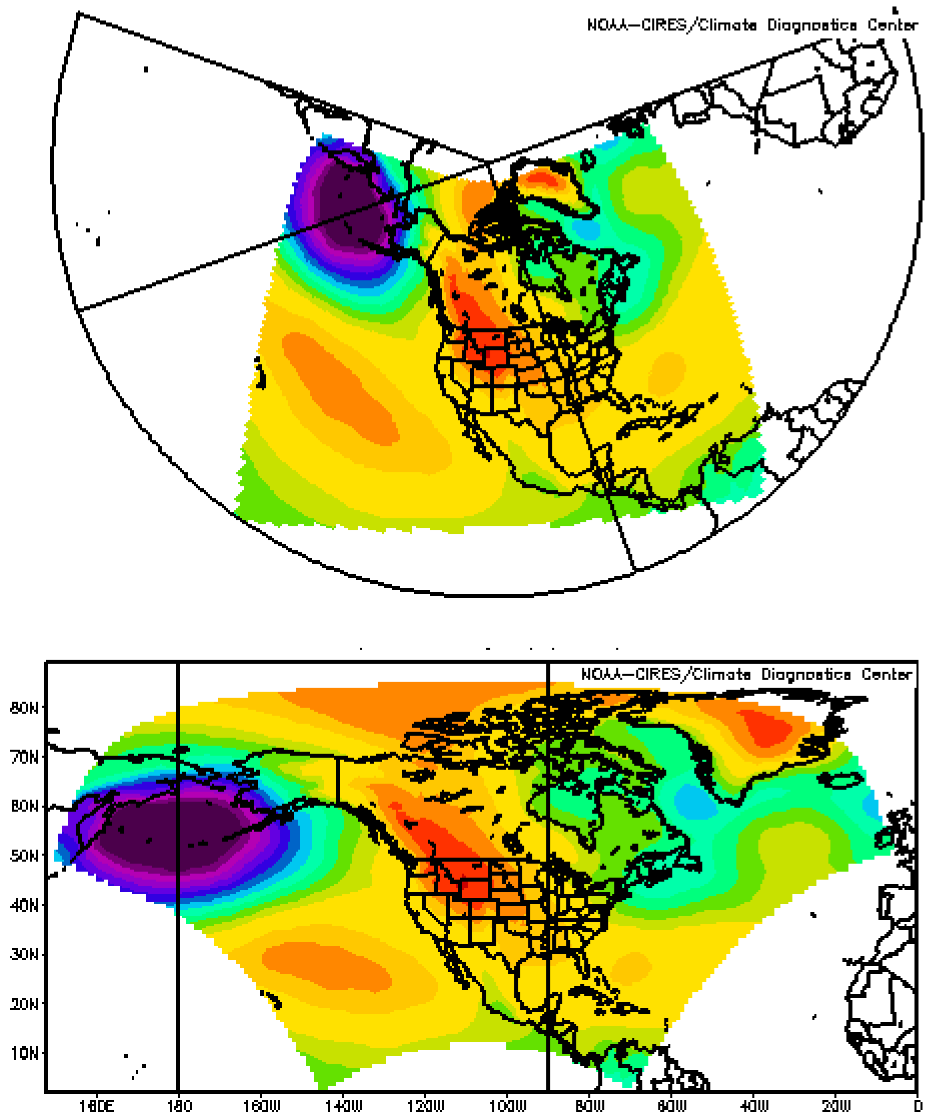

Fig. 3.11. NARR model *sample* data (a) projected onto 349 x 277 Lambert Conformal Conic grid and (b) the latitude/longitude associated with the coordinate pairs.

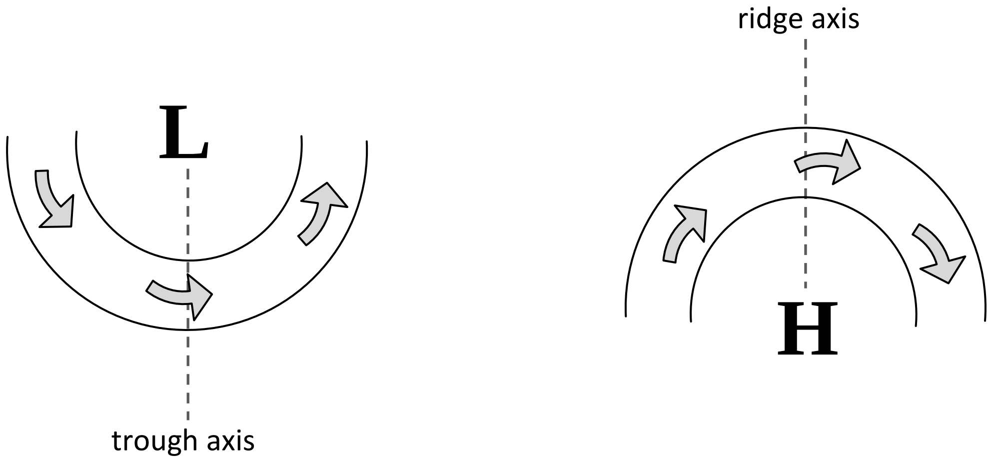

Fig. 3.12. Illustration of a synoptic scale "trough and ridge" pattern. Troughs are associated with lower pressure and cooler temperatures than ridges.

CHAPTER 4

RESULTS

4.1 Quantifying Tornado Days

4.1.1 *Drought Periods*

Palmer *Z*-index and normalized soil moisture are correlated using Pearson's product-moment correlation coefficient to assess how well soil moisture alone defines drought periods. The coefficient is a measure of the linear dependence between two variables. The results are shown in Table 4.1. It should be noted that the *Z*-index is not a direct measure of soil moisture content and thus is not expected to correlate perfectly with normalized soil moisture (Dai et al 2004), but will help determine if normalized soil moisture captures the majority of drought periods. The 6-month normalized soil moisture most consistently correlates with the *Z*-index as hypothesized and will be used as the sole antecedent period for the majority of the tornado analyses. An interesting finding of this analysis is the correlation coefficients increase eastward from Alabama Climate Zone 1. Further investigation is beyond the scope of this paper, but it is speculated that land cover and vegetation affect the Palmer *Z*-index more so than the normalized soil moisture. A land cover map (Fig. 4.1) and canopy map (Fig. 4.2) are provided to show how land cover changes across the study area. Georgia climate division 2 contains Atlanta, a highly developed area. Georgia divisions 1 and 3 are mostly a mix of forest and pasture/hay. Alabama divisions 1 and 3 contain highly developed areas, open water, and pasture/hay. Alabama division 3 contains wetlands and forest. Forest canopy is the most dense over central Alabama and northeastern Georgia.

4.1.2 *Percent of Normal Tornado Days*

A scatterplot of normalized soil moisture and tornado days is used to analyze the relationship between drought periods and strength of the following tornado season. The plot clearly reveals that significantly negative antecedent soil moisture departures (e.g., drought) are almost always associated with below normal tornado days during spring (Fig. 4.3). A statistical T-Test of the coefficient shows a moderate positive correlation ($R = 0.34$) significant at the 95% confidence level ($p = 0.041$). Table 4.2 summarizes the attributes of all drought and all non-drought years. The six years defined as drought (*z*-score < -1.0) are all associated with equal to or below normal tornado days. Drought years have an average of 4.17 tornado days per tornado season, while non-drought years have an average of 5.19 tornado days per tornado season. The results presented herein are extremely consistent with results reported in Shepherd et al. (2009) although different methods and data (e.g. precipitation-driven soil moisture rather than precipitation departure) over a larger area were applied. The results clearly show that when antecedent drought is present in the study area, below normal tornado days characterize the following spring season. As in Shepherd et al. (2009), these results also show that more tornado days are associated with non-drought antecedent years. However, there seems to be a consistent signal when very dry or drought conditions are present. The consistency of the results herein and those of Shepherd et al. (2009) suggest that at least for the southeastern United States, there may be seasonal predictive capacity for tornado days when drought is present the previous season.

These results are also consistent to others that indicate an asymmetry in the influence of soil moisture. Oglesby et al. (2002), using NCAR CCM3, reported that dry anomalies had larger impacts on the precipitation feedback than wet anomalies in the central United States. Bosilovich and Schubert (2001) show the recycling ratio in the central United States was above average in the dry summer of 1988 and below average in the wet summer of 1993, suggesting soil moisture exerts more influence on the atmosphere during droughts than floods.

4.1.3 *Tornado Tracks*

The geographic distribution of tornado tracks for drought and non-drought years, respectively, are analyzed for significant differences and characteristics. This analysis seems to be unique in that nothing similar has been found in past literature. The composite tornado track maps for drought and non-drought cases are shown in Fig. 4.4. The number of “tornado season” tornadoes that occur under antecedent drought conditions is 72, while tornadoes during antecedent high soil moisture conditions total 100.

In addition to an overall higher count, non-drought years have F0 to F5 tornado reports while drought years contain only F0 to F3 (Fig. 4.5). Drought year tornadoes have an average length of 5.14 miles and average width of 67 yards. Non-drought year tornadoes have an average length of 5.2 miles and an average width of 74 yards. This suggests antecedent drought reduces the likelihood of extremely violent tornadoes and is characterized by shorter and narrower tornado tracks in the spring. While the sample was somewhat limited, the results are interesting and warrant additional study.

An "average nearest neighbor" analysis is done on the drought and non-drought composite maps. Table 4.3 shows the results of the analysis. For the non-drought map, the observed mean distance between the tornado tracks is 0.203 decimal degrees compared to the drought tornado track mean distance of 0.256 decimal degrees. This suggests during antecedent drought conditions, tornado tracks are further apart than during non-drought conditions, possibly due to less tornado occurrences overall, shorter tracks, or different spatial distributions. Note, however, these results are not considered conclusive as only six years were used for each composite. An anomalously intense tornado season could easily skew the results.

4.2 Convective Parameters

4.2.1 *Composite Maps*

There is evidence of a correlation between tornadoes and antecedent soil moisture shown in the previous sections. Shepherd et al. (2009) suggested that a possible relationship might exist between instability measures (CAPE and CIN) and antecedent soil moisture. The objective here is to see if soil moisture conditions have any consistent relationship to the instability of the atmosphere that would affect tornado activity in the spring. Composite maps of 1-month antecedent CAPE and CIN are analyzed during drought and non-drought years (Fig. 4.6). The drought composite shows CAPE is consistently lower than in the non-drought composite over the study area. In both cases CAPE values decrease to the northeast. To better compare the two maps, a difference map is created by subtracting the drought years from the non-drought years (Fig. 4.7). It shows the CAPE values over the domain are positive, or the non-drought composite has a higher mean CAPE than the drought composite. Of 336 grid points in the domain, the non-drought composite CAPE is greater than drought composite CAPE at 303 points (90.2%). Alonge et al. (2006) found domain-averaged CAPE is higher for wet soil moisture regimes than dry soil moisture regimes on a convective activity day. Clark and Arritt (1995) found the combined sensible and latent heat fluxes over saturated, bare soil are higher than those over dry, bare soil, resulting in more boundary layer moisture and higher CAPE.

The spatial distribution of mean CIN during February resulted in similar findings. The drought years have more negatively buoyant energy. In both drought and non-drought years, CIN becomes more negative towards the southwest part of the study area (Fig. 4.8). Even with these findings, the magnitudes of difference likely do not explain the observed differences in convective activity. A CAPE and CIN distribution for the area-averaged values over the 27-year period is shown in Table 4.4. CAPE values range from 4.04 to 80.77 $J \cdot kg^{-1}$. CIN values range from -0.92 to -14.82 $J \cdot kg^{-1}$. These values are much smaller than the operational significance since they are averaged spatially and temporally.

Composite maps for CAPE and CIN during the tornado season are used to better understand the magnitude of the values. Fig. 4.9 shows the CAPE composite maps during the spring tornado season for (a) drought and (b) non-drought years. The CAPE values during this period are larger than during the month of February. Similar to February, the non-drought composite has overall higher values than the drought composite in the spring. Fig. 4.10 displays the CIN composite maps during the tornado season for (a) drought and (b) non-drought years. Again, the CIN values are more extreme during the tornado season compared to the 1-month antecedent period. However, non-drought years have more CIN than the drought years, opposite to the findings for February.

To continue the convective-drought analysis, CAPE and CIN data are normalized using the *z*-score method and then compared to normalized soil moisture using scatterplots. The scatterplots for both analyses can be seen in Fig. 4.11. The CAPE plot does not show an obvious trend for above normal soil moisture. Above normal soil moisture does tend to correspond to more extreme positive CAPE anomalies than negative CAPE anomalies. Below normal soil moisture almost always corresponds to negative CAPE anomalies. For both above and below normal soil moisture, the negative CAPE anomalies are within 1.5 standard deviations. This analysis agrees with the findings of previous work where below normal soil moisture results in lower CAPE, yet high soil moisture does not seem to show any distinct signal (see section 4.1.2).

The CIN plot indicates above normal soil moisture almost always corresponds with positive CIN anomalies. Below normal soil moisture corresponds to positive CIN anomalies slightly more often than negative anomalies. For both above and below normal soil moisture, the negative CIN anomalies are more extreme (within 3 standard deviations) while the positive CIN anomalies are within 1 standard deviation. The correlation between normalized CAPE and soil moisture is not significant at the 95% confidence level ($R=0.183$) nor is normalized CIN and soil moisture ($R=0.094$).

Generally, the CAPE/CIN analyses proved to be somewhat inconclusive and somewhat problematic: (1) the magnitude of the CAPE and CIN differences are relatively small, and (2) it was not clear that they could explain the observations related to tornadic storms. Furthermore, the methodology was somewhat flawed in that antecedent CAPE/CIN values may be meaningless when considering convective activity during the spring. A more explicit analysis of soil moisture memory and its persistence is described in section 4.3.

4.2.2 *Synoptic Conditions*

It is hypothesized that the convective parameter-soil moisture relationship may be a function of large-scale synoptic patterns on a climatological scale. In discussions with Joe Schaeffer (Shepherd, personal communication, 2009), director of NOAA’s Storm Prediction Center (SPC), he suggested that the results of Shepherd et al. (2009) may be related to differences in the upper level forcing. Fig. 4.12 shows the 1-month antecedent 500 hPa geopotential heights composited for (a) non-drought and (b) drought years, respectively. The maps show a slight large-scale difference in synoptic patterns between drought and non-drought cases. A difference map between drought and non-drought years during the 1-month antecedent period is shown in Fig. 4.13. The 500 hPa level over the Southeast is 40 to 50 m higher during drought years. Because the drought composite has more ridging and slightly higher pressure, it may be forcing the fall/winter soil moisture conditions into the spring. This moisture persistence may account for the tornado day difference between wet and dry regimes and is discussed in the following section.

4.3 Soil Moisture Persistence

4.3.1 *Correlation*

Because the convective parameters did not significantly correlate to antecedent soil moisture, a more direct method of quantifying the soil moisture memory effect is used by comparing the 6-month antecedent soil moisture to spring (March, April, May) soil moisture. This analysis indicates how persistent soil moisture conditions are for antecedent drought and non-drought cases, respectively. The hypothesis is anchored to the notion of precipitation and moisture recycling. Precipitation recycling is an understanding of the water cycle from an atmospheric viewpoint (Fig. 4.14). On a regional scale, there is probability that a water molecule evaporated at the surface will precipitate within the same region. Two important components that characterize the regional water cycle are locally recycled water vapor molecules and atmospheric water vapor transported from outside the region (Eltahir and Bras 1996). Herein, this notion is extended to assume that soil moisture persistence can be represented by the same framework. Pearson's correlation analysis reveals that normalized soil moisture is somewhat more persistent during drier conditions than high soil moisture conditions. Table 4.5 lists the correlation coefficients for several subsets of years. The correlation coefficient is highest for "all years" because of the increased number of years compared to the subsets of years.

4.3.2 *Scatterplot*

A closer look at the soil moisture memories reveals some very interesting results. A soil moisture persistence scatterplot is evaluated to see if drought conditions in fall/winter are a good predictor of drier soil moisture conditions the following spring. Fig. 4.15 shows (a) the labeled quadrants based on antecedent soil moisture on the x-axis and spring soil moisture on the y-axis and (b) the scatterplot of the soil moisture values 1980-2006. Six-month antecedent drought values are outlined in red. An important result from this analysis is when the antecedent fall/winter soil moisture is very dry (< -1.0 normalized soil moisture departure), such conditions are extremely likely to persist into the spring. Since our previous results associate drought with reduced tornado days, this suggests that extremely dry antecedent drought fall/winter periods are very good indicators of below normal tornado days the following spring. Guidelines for predicting spring soil moisture from antecedent conditions are summarized in Table 4.6.

The values tend to cluster in quadrants I, II, and III. The driest antecedent periods (below -1 standard deviation) correspond to the driest spring values, while marginally dry to normal years correspond to either dry or wet springs. The wettest antecedent periods are almost always associated with wet springs. The dry soil results agree with previous literature, however the wet soil results are more surprising. Pal and Eltahir (2001), Oglesby et al. (2002), Bosilovich and Schubert (2001), and Meng (2009) all state that dry soil has a more lasting memory than wet soil. It would be expected that wet antecedent soil does not have a predictable spring soil moisture anomaly, as also suggested by the tornado day analysis (section 4.1.2) and CAPE correlation analysis (section 4.2). In summary, the results strongly suggest that the physical mechanism that may be most associated with the linkage between antecedent fall/winter drought and spring tornado day reduction is the persistence of dry soil from the driest antecedent periods. The results also suggest that for marginally dry to wet antecedent conditions, there is less predictability of the spring soil moisture conditions. This may be due to the soil characteristics or climatology of the southeastern United States. Upper-level ridging may be driving seasonal soil moisture persistence.

As mentioned in Meng (2009), the water holding capacity of the soils in the study area can have an effect on how easily soil moisture is replenished. Fig. 4.16 categorizes the water holding capacity of soils in the U.S. The majority of the study area has “moderate” holding potential, which is 25-100 mm of water.

4.4 Bermuda High Index

4.4.1 *Fall/Winter BHI*

Because this research is focused on antecedent drought periods, the last objective is to gain an understanding of the relationship between southeastern United States fall/winter drought periods and the Bermuda High. This research extends Doublin and Grundstein's (2008) work, which focused primarily on the warm season. Henderson and Vega (1996) and Doublin and Grundstein (2008) documented that a Bermuda High system situated over the Atlantic Ocean brings strong southerly flow and precipitation to the southeastern United States. The BHI is therefore selected as the most appropriate large-scale oscillation to link to drought in this research. The BHI is calculated for the 1- and 6-month antecedent periods and plotted against normalized soil moisture. Fig. 4.17 illustrates the time series plot and Fig. 4.18 the scatterplot of 6-month antecedent BHI (MSLP averaged September-February) versus the 6-month normalized soil moisture. There is not a significant positive correlation between the two variables at the 95% confidence level (R = 0.25). Looking at just the sign of the BHI phases and not the magnitude, antecedent drought years based on 6-month normalized soil moisture correspond to a negative BHI 5 of out 6 years (83.3%) (Table 4.7).

Fig. 4.19 shows the time series and Fig. 4.20 the scatterplot of 6-month BHI versus the 1-month normalized soil moisture. A T-Test indicates there is a significant positive correlation at the 95% confidence level (R = 0.34). Similarly, drought years based on 1-month normalized soil moisture corresponded to a negative BHI 4 out of 6 years (66.7%) (Table 4.8). These results suggest the Bermuda High during fall/winter may have some influence on the soil moisture conditions during the same period. This is consistent with Doublin and Grundstein (2008) who found that the warm season BHI was associated with drought during that same period.

4.4.2 *Warm Season BHI*

Since the BHI is considered a warm season phenomena, analysis is also carried out for an earlier period, MSLP averaged over the period May-September (e.g., the warm season leading up to the fall/winter antecedent period for the following spring). Fig. 4.21 contains a time series plot and Fig. 4.22

a scatterplot of warm season BHI versus 6-month normalized soil moisture. Fig. 4.23 contains a time series plot and Fig. 4.24 a scatterplot of warm season BHI versus 1-month normalized soil moisture. There is not a significant positive correlation for warm season BHI and 6-month normalized soil moisture (R = 0.20) nor any correlation with 1-month normalized soil moisture (R = 0.00). Drought years correspond to negative BHI only 3 of 6 years (50%). These results indicate the warm season BHI does not have much association with the following fall/winter drought.

4.4.3 *Rank Analysis*

The correlation analyses did not reveal any conclusive relationships between the magnitude of the BHI and drought years. Therefore, an association test may be more useful for the two datasets. A rank analysis and sign test is used to match positive (negative) signs of BHI and normalized soil moisture (all years).

For warm season BHI, 6-month normalized soil moisture is below normal 62.5 % of the years that BHI is negative (the negative signs match 10 of 16 years). One-month normalized soil moisture is below normal 56.3 % of the years that BHI is negative (9 of 16 years).

For fall/winter BHI, 6-month antecedent soil moisture and BHI match signs 7 of 13 years that soil moisture is negative. BHI is negative 7 of 14 years that February soil moisture is below normal. This suggests, together with section 4.4.1, that negative fall/winter BHI occurs in almost all drought years, but not necessarily below normal soil moisture years in general. Warm season BHI does not seem to correlate to drought or below normal soil moisture during the fall/winter nor February alone.

In summary, results from objective 1 show 6-month normalized soil moisture most consistently correlate with the Palmer Z-index in terms of drought conditions, drought periods are almost always associated with below normal tornado days during spring, and more tornadoes occur during the six wettest years than the six drought years. Results from objective 2 reveal CAPE is lower and CIN is higher in the drought years composite. Scatterplots indicate below normal soil moisture results in lower CAPE, yet high soil moisture does not seem to show any distinct signal. CIN has similar values for both above and below normal soil moisture. There is a slight large-scale difference in synoptic patterns between drought and non-drought cases, as the drought composite shows more ridging. Objective 3 results indicate drought periods correspond to the driest spring values, while marginally dry to normal years correspond to either dry or wet springs. The wettest antecedent periods are almost always associated with wet springs. Objective 4 correlation results suggest the Bermuda High during fall/winter may have some influence on the soil moisture conditions during the same period. Association analysis reveals negative fall/winter BHI occurs in almost all drought years, but not necessarily below normal soil moisture years in general. The conclusions of these results are presented in Chapter 5.

Table 4.1. Pearson's product-moment correlation coefficients.

	Climate Division					
Period	AL Zone 1	AL Zone 2	AL Zone 3	GA Zone 1	GA Zone 2	GA Zone 3
1-Month	0.36	0.37	0.37	0.41	0.55	0.56
2-Month	0.24	0.36	0.39	0.46	0.58	0.68
6-Month	0.51	0.53	0.58	0.62	0.56	0.58

Table 4.2. Attributes of drought and non-drought years.

	Drought years only	Non-drought years only
Number of years	6	21
Mean number of tornado days (Mar-May)	4.17	5.19
Mean number of multiple tornado days (Mar-May)	2.17	2.90
Years with above normal tornado days (%)	0	38.1
Years with below-normal tornado days (%)	100	61.9

Table 4.3. Average nearest neighbor results.

	Non-drought	Drought
Observed Mean Distance	0.20	0.26
Expected Mean Distance	0.21	0.24
Nearest Neighbor Ratio	0.94	1.06

Table 4.4. Area-averaged February CAPE and CIN value distribution 1980-2006 for the Southeast.

Percentile	CAPE Value ($J \cdot kg^{-1}$)	CIN Value ($J \cdot kg^{-1}$)
25^{th}	15.38	-2.14
50^{th}	22.07	-3.75
75^{th}	29.41	-5.59
90^{th}	54.03	-9.67
99^{th}	76.30	-14.38

Table 4.5. Pearson's correlation coefficient for 6-month antecedent and spring normalized soil moisture.

Period	Correlation Coefficient
Drought years	0.15
Six wettest years	0.06
Below normal soil moisture	0.23
Above normal soil moisture	0.19
All years (1980-2006)	0.65

Table 4.6. Predicted spring soil moisture based on 6-month antecedent soil moisture.

Fall/winter normalized soil moisture departure	Quadrant(s)	Predicted spring soil moisture conditions
< -1.0	III	Dry
-1.0 – 0.0	I & III	Dry or Wet
> 0.0	II	Wet

Table 4.7. Z-score values and sign agreement for fall/winter soil moisture and fall/winter BHI.

Drought Years	Soil Moisture	BHI	Sign Agreement?
1981	-1.11	-1.54	yes
1982	-1.19	-1.05	yes
1988	-1.29	-0.71	yes
1989	-1.11	0.23	no
2000	-1.61	-0.19	yes
2001	-1.82	-0.88	yes

Table 4.8. Z-score values and sign agreement for February soil moisture and fall/winter BHI.

Drought Years	Soil Moisture	BHI	Sign Agreement?
1981	-1.64	-1.54	yes
1986	-1.15	1.07	no
1988	-1.19	-0.71	yes
1989	-1.31	0.23	no
2000	-2.04	-0.19	yes
2001	-1.65	-0.88	yes

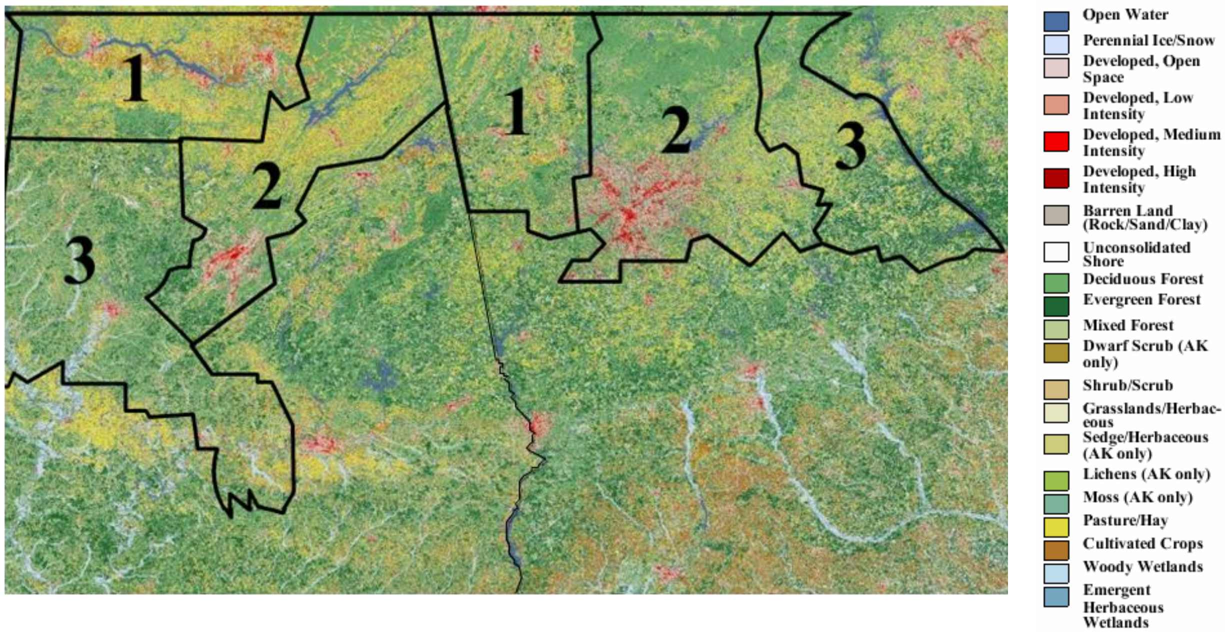

Fig. 4.1. USGS Land cover map with climate zones.

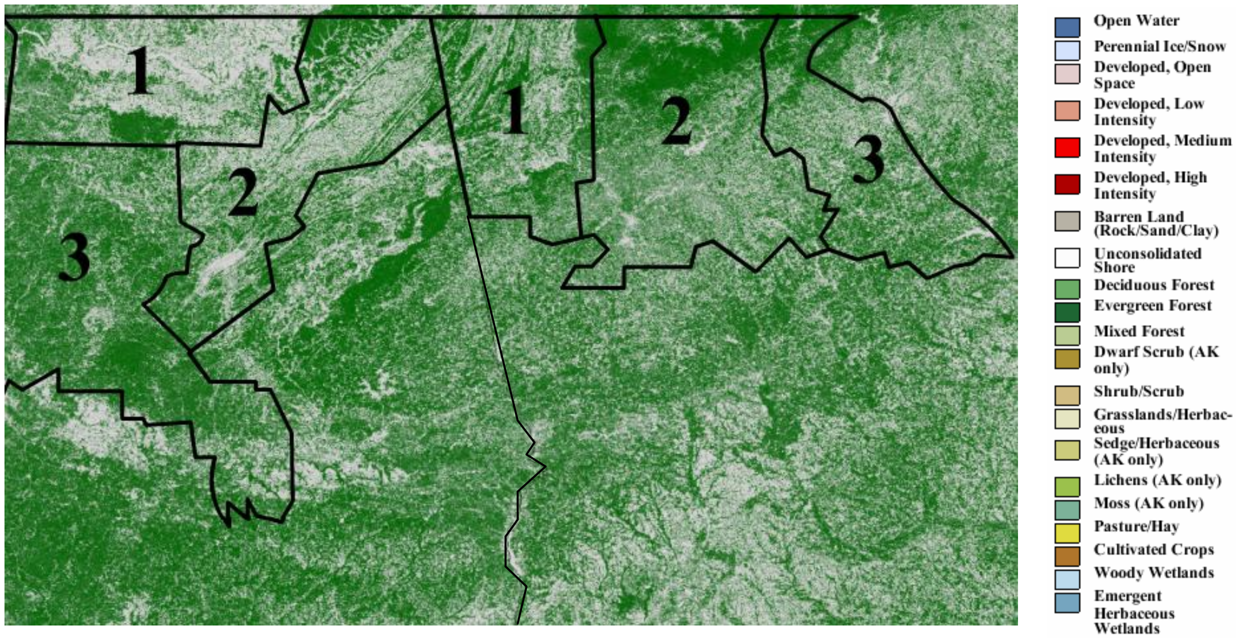

Fig. 4.2. USGS canopy map with climate zones.

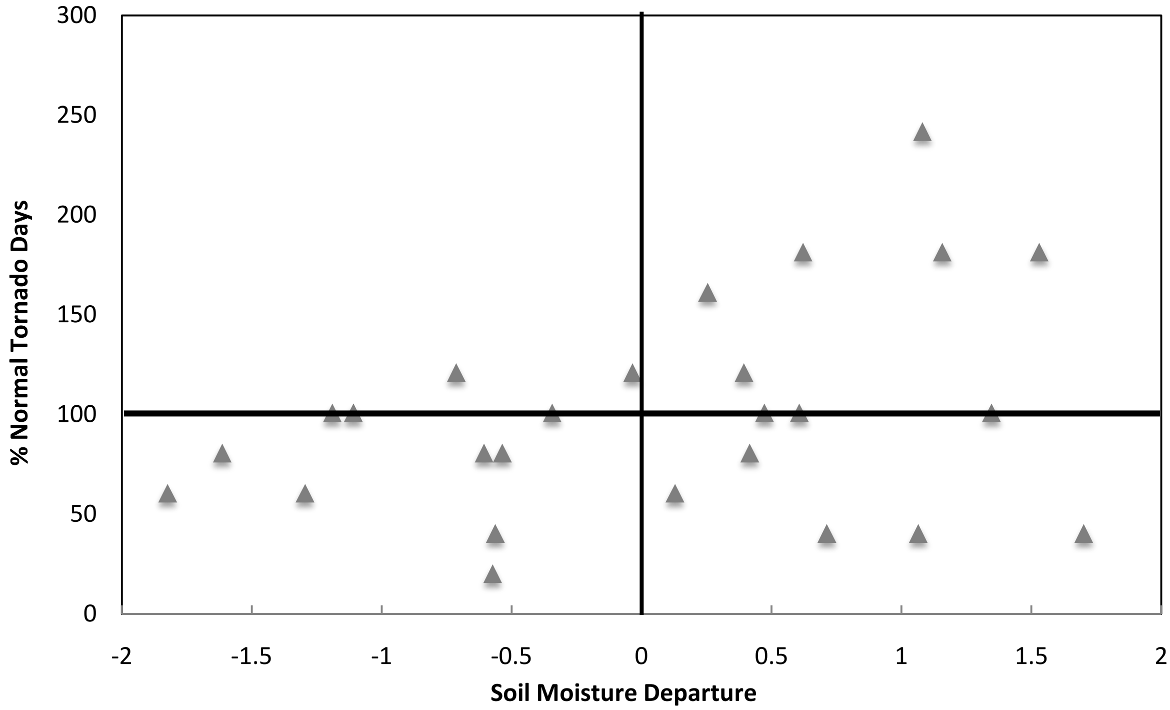

Fig. 4.3. Relationship between normalized tornado days and 6-month antecedent soil moisture 1980-2006. The vertical line is normal tornado days (per tornado season) while the horizontal line is normal soil moisture.

(a)

(b)

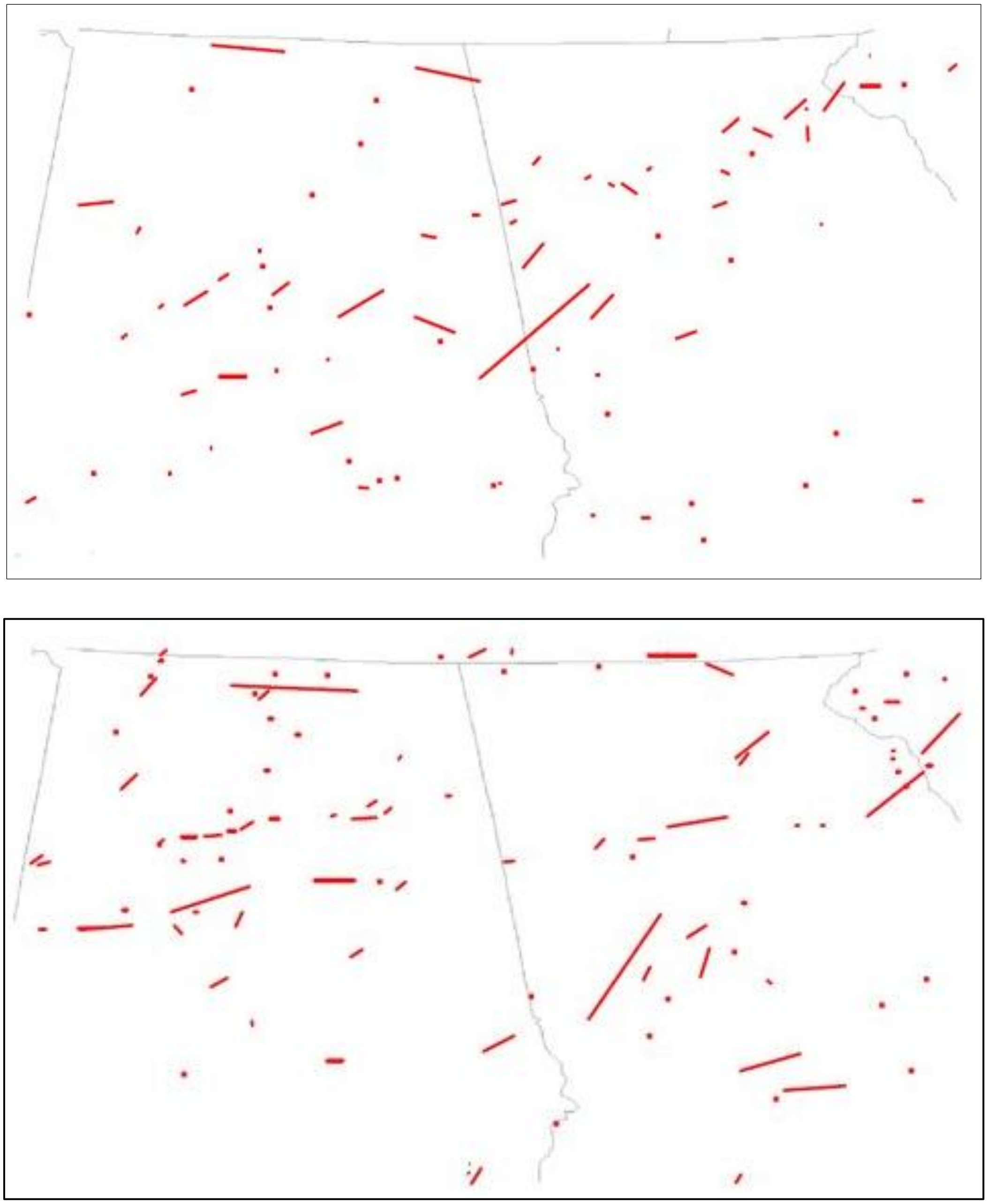

Fig. 4.4. Composite tornado tracks for (a) antecedent drought and (b) non-drought years. The number of "tornado season" tornadoes that occur under antecedent drought conditions is 72, while tornadoes during antecedent high soil moisture conditions total 100.

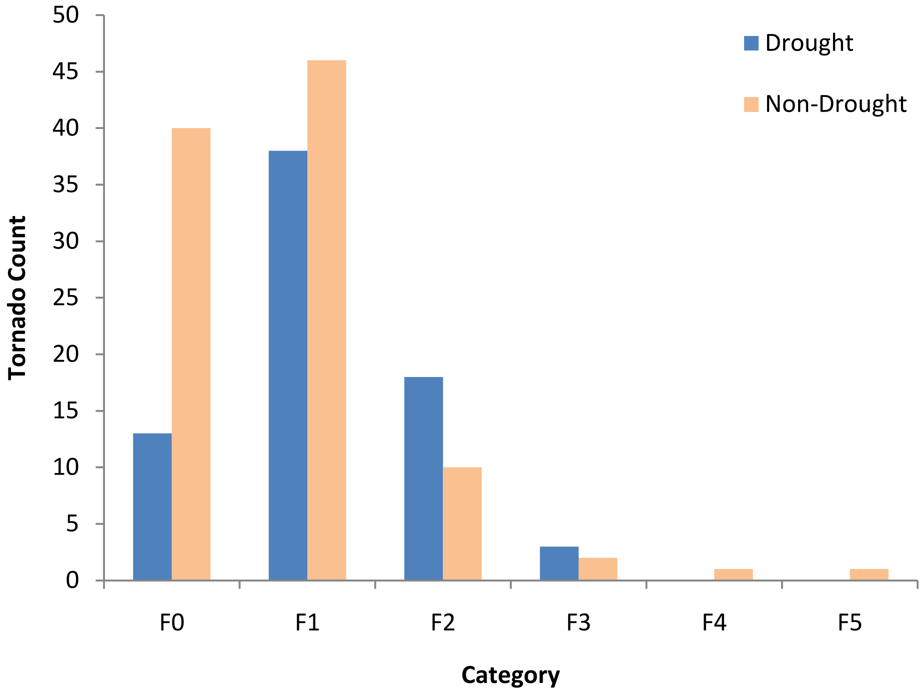

Fig. 4.5. Tornado counts during the tornado season for drought years (blue) and non-drought years (orange).

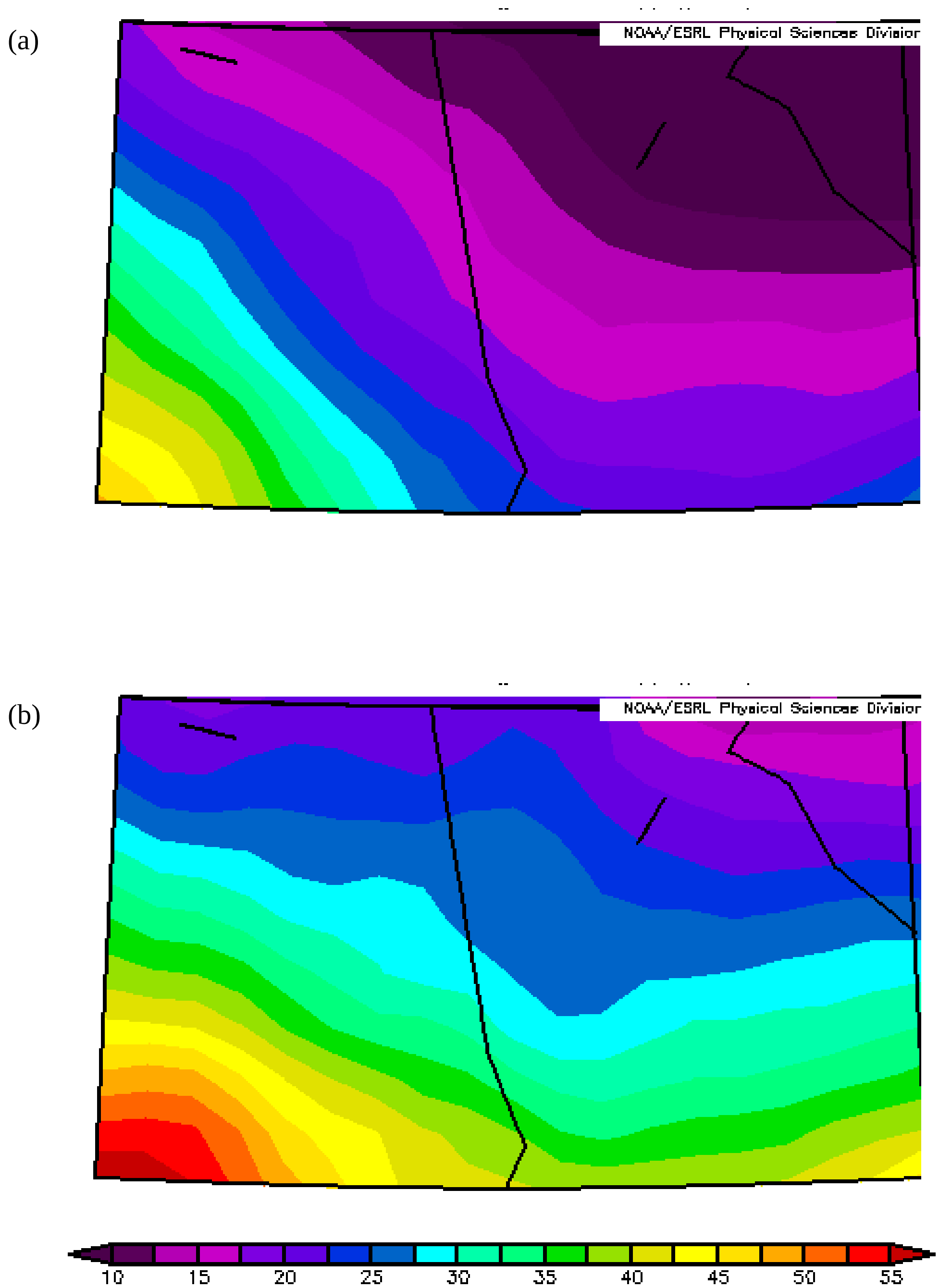

Fig. 4.6. Composite CAPE (J/kg) during February for (a) drought years and (b) non-drought years. CAPE is consistently lower during antecedent drought than in the non-drought composite.

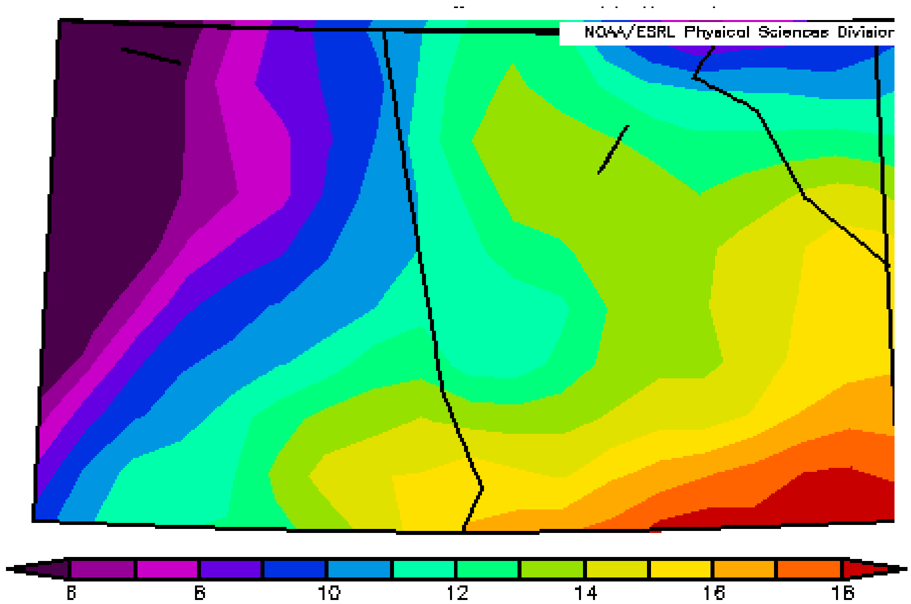

Fig. 4.7. Difference between drought and non-drought composite mean for February. The CAPE values over the domain are positive, or the non-drought composite has a higher mean CAPE than the drought composite. Of 336 grid points in the domain, the non-drought composite CAPE is greater than drought composite CAPE at 303 points (90.2%)

(a)

(b)

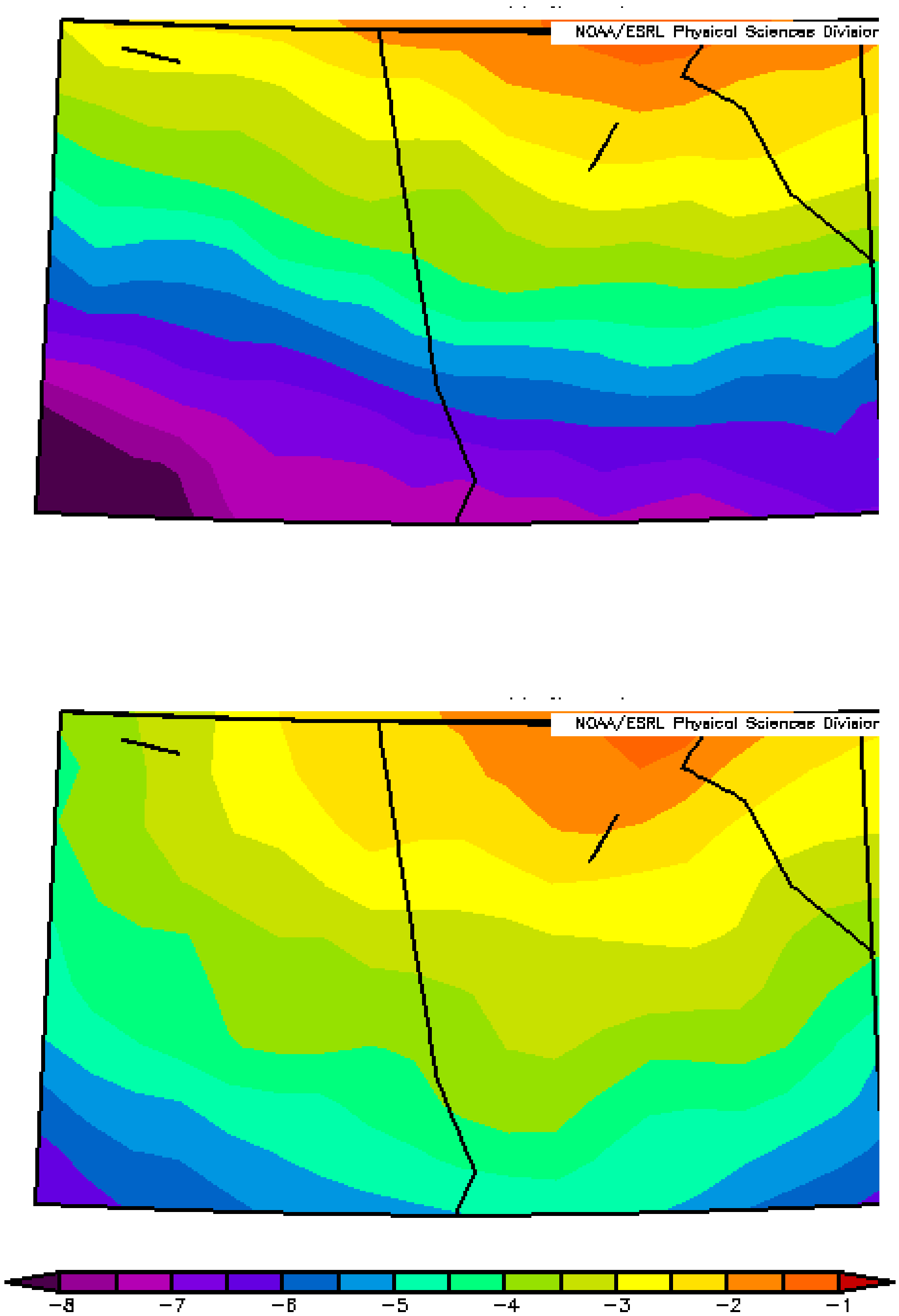

Fig. 4.8. Composite mean Convective Inhibition at surface (J/kg) for February during (a) drought years and (b) non-drought years. The drought years have more negatively buoyant energy.

(a)

(b)

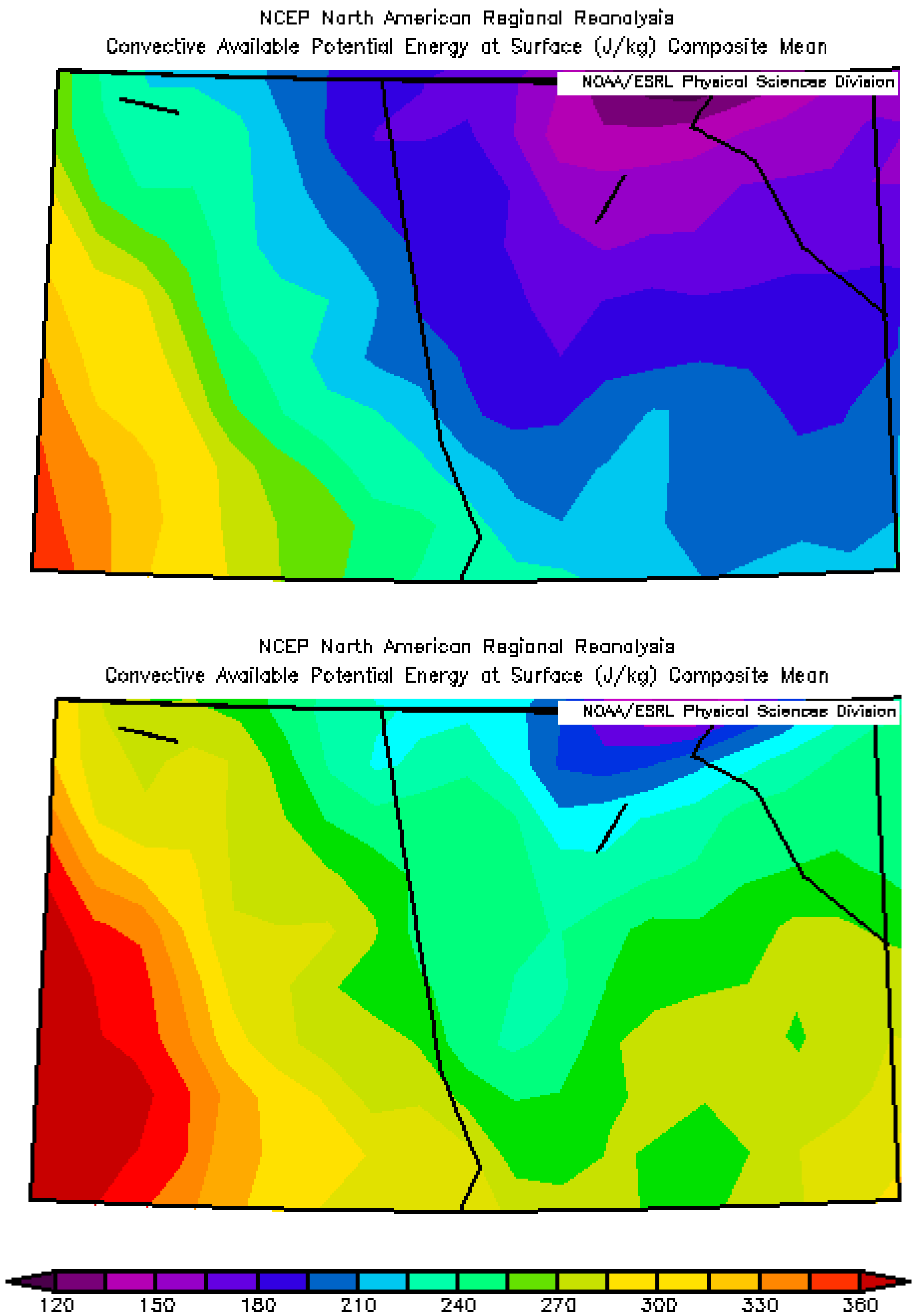

Fig. 4.9. Composite CAPE map (March-May) during antecedent (a) drought and (b) non-drought.

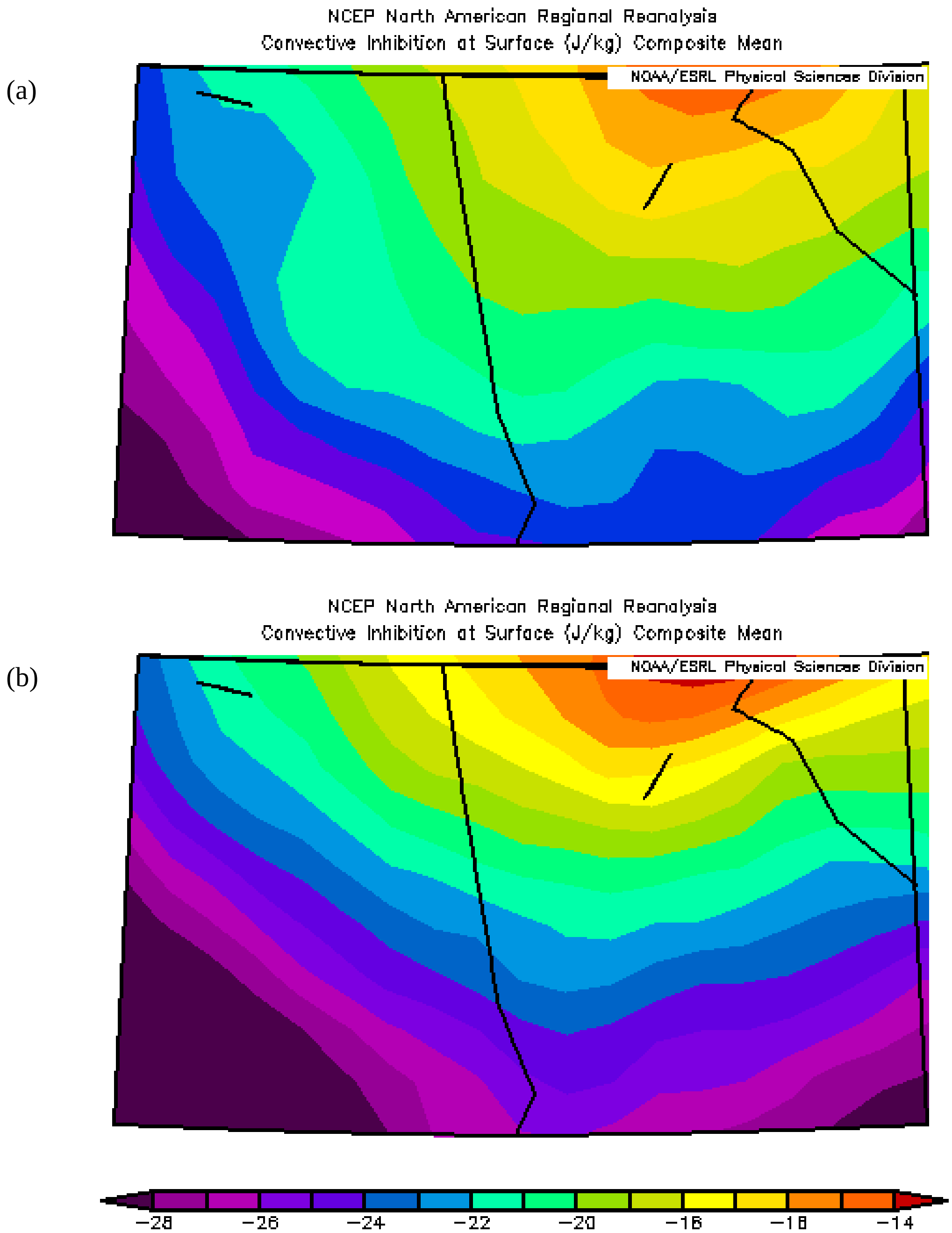

Fig. 4.10. Composite CIN map (March-May) during antecedent (a) drought and (b) non-drought.

(a)

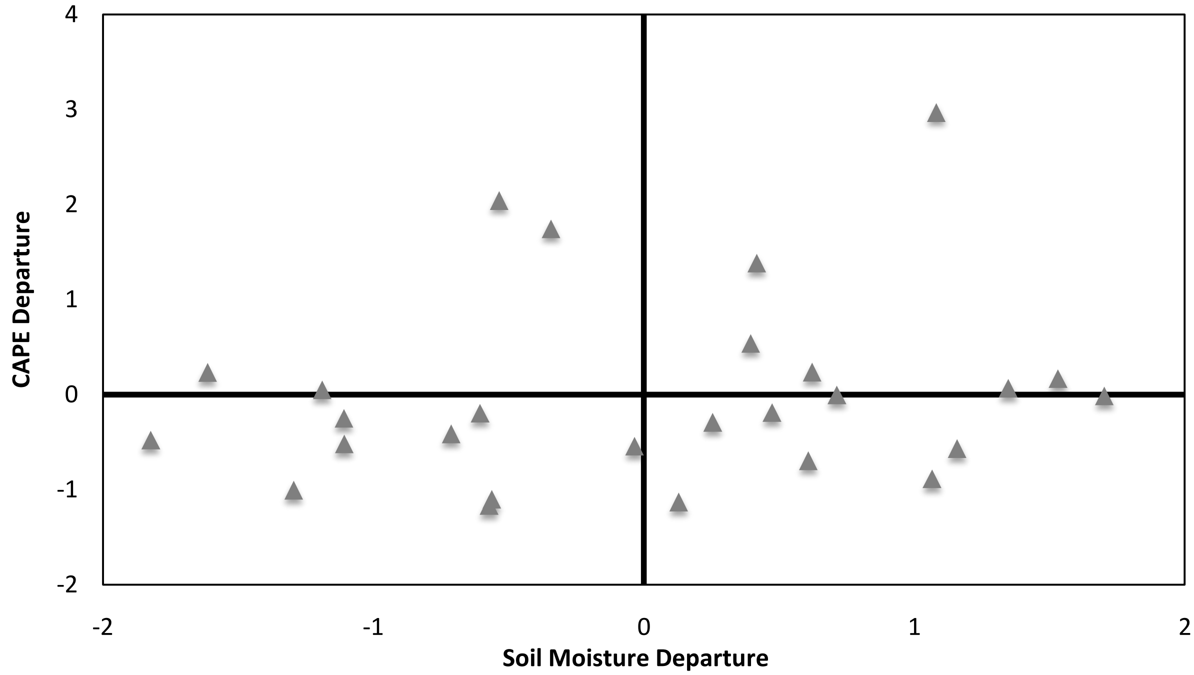

(b)

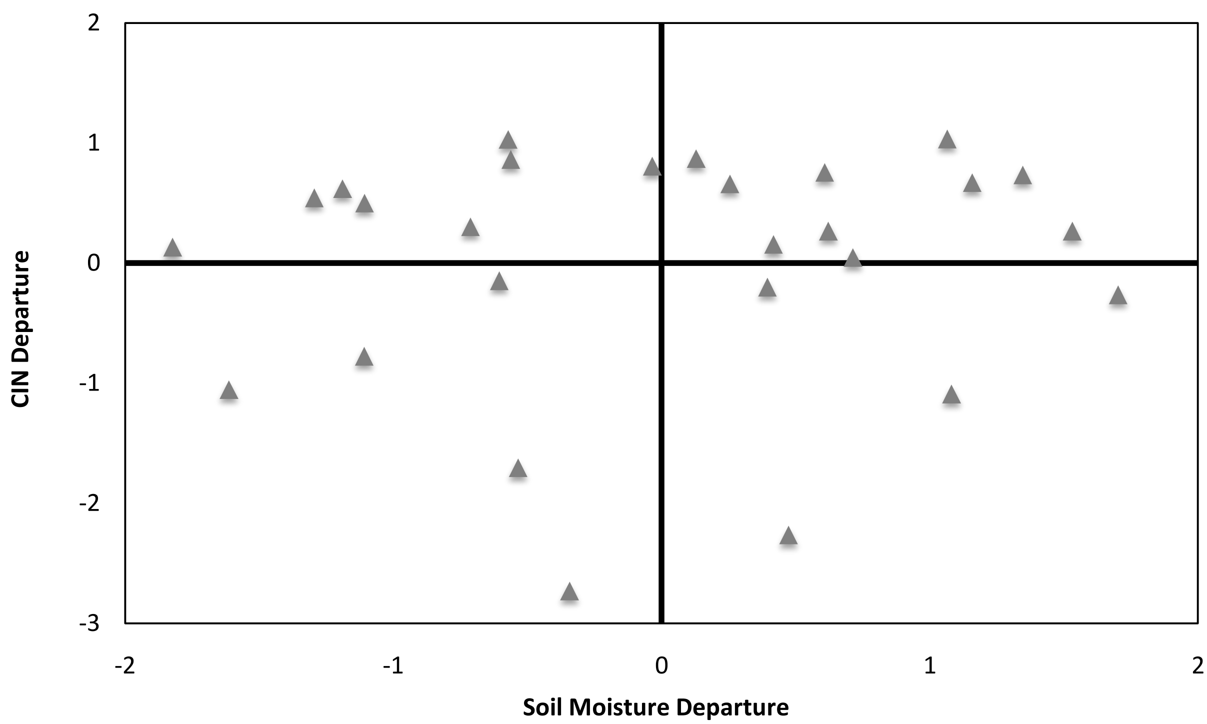

Fig. 4.11. Normalized (a) CAPE and (b) CIN correlated to normalized soil moisture (1980-2006). Below normal soil moisture results in lower CAPE, yet high soil moisture does not seem to show any distinct signal.

(a)

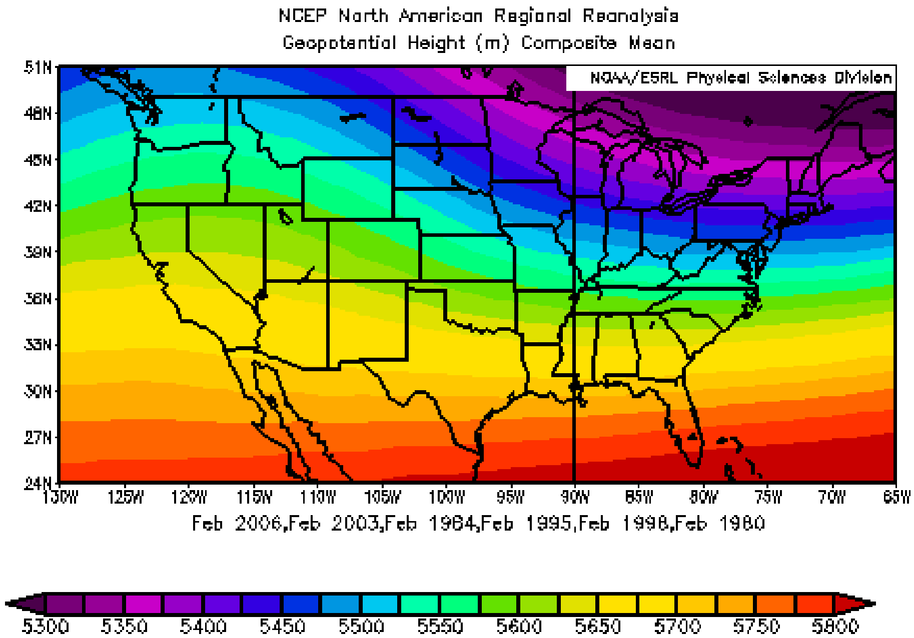

(b)

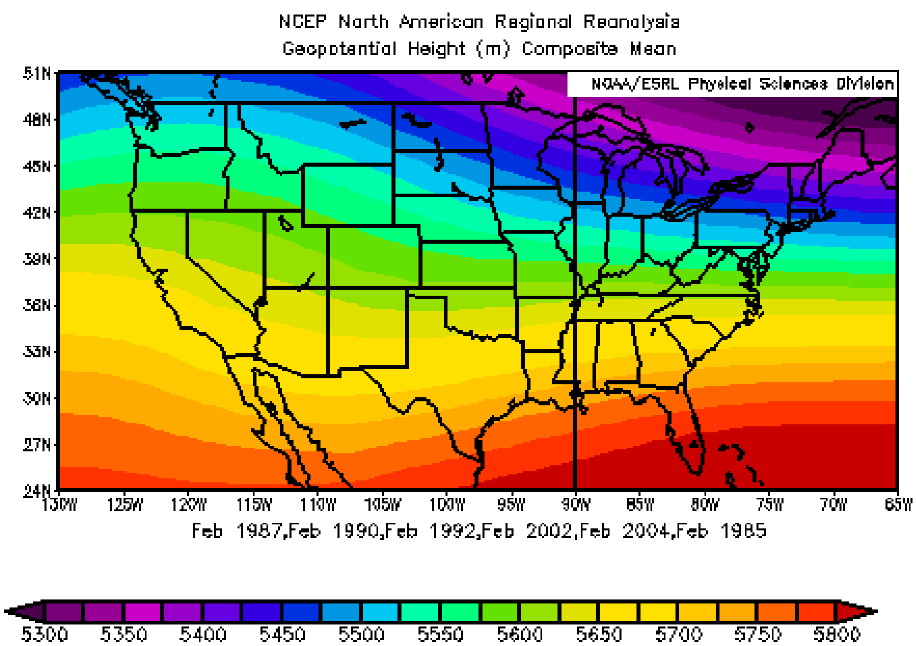

Fig. 4.12. Composite 500 hPa geopotential heights for (a) non-drought years and (b) drought years during the 1-month antecedent period. Units are in meters.

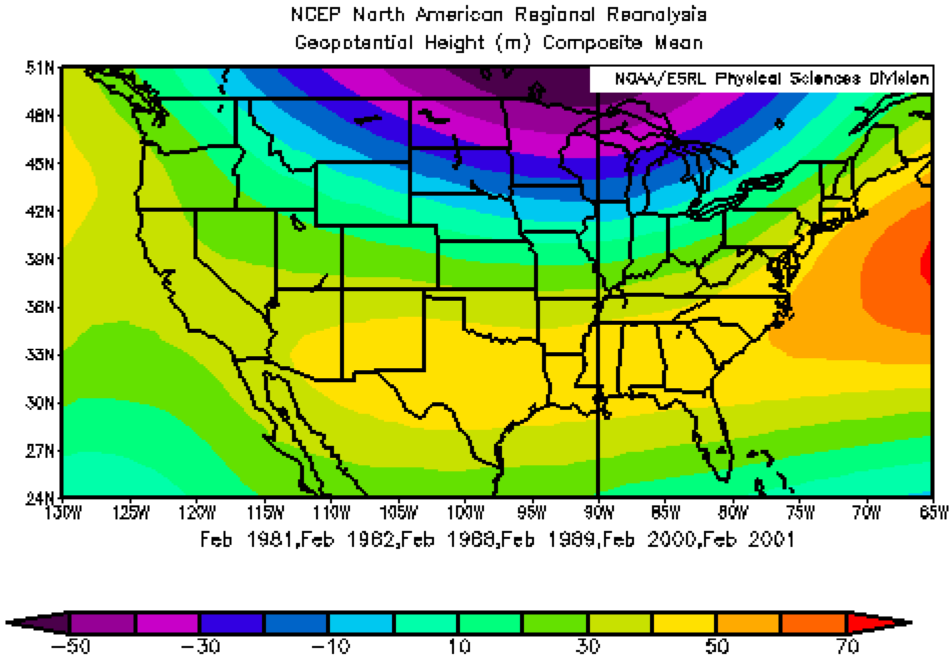

Fig. 4.13. Composite 500 hPa difference map between drought and non-drought years during the 1-month antecedent period. The 500 hPa level over the Southeast is 40 to 50 m higher during drought years.

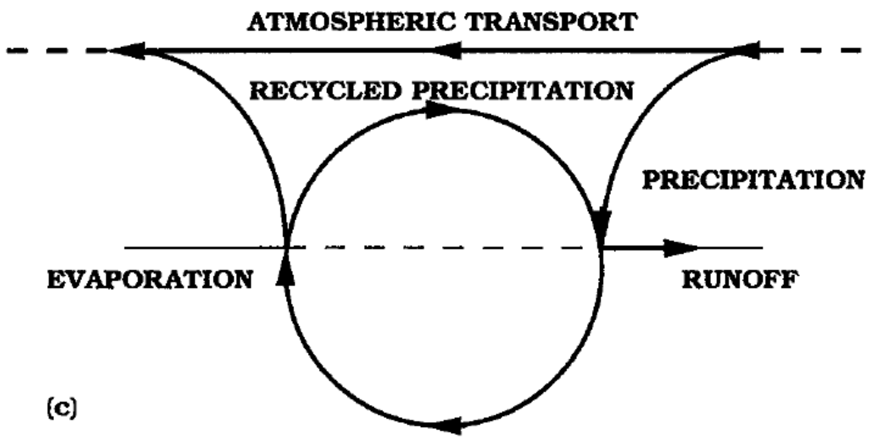

Fig. 4.14. Schematic of the regional hydrologic cycle and precipitation recycling (from Eltahir and Bras 1996).

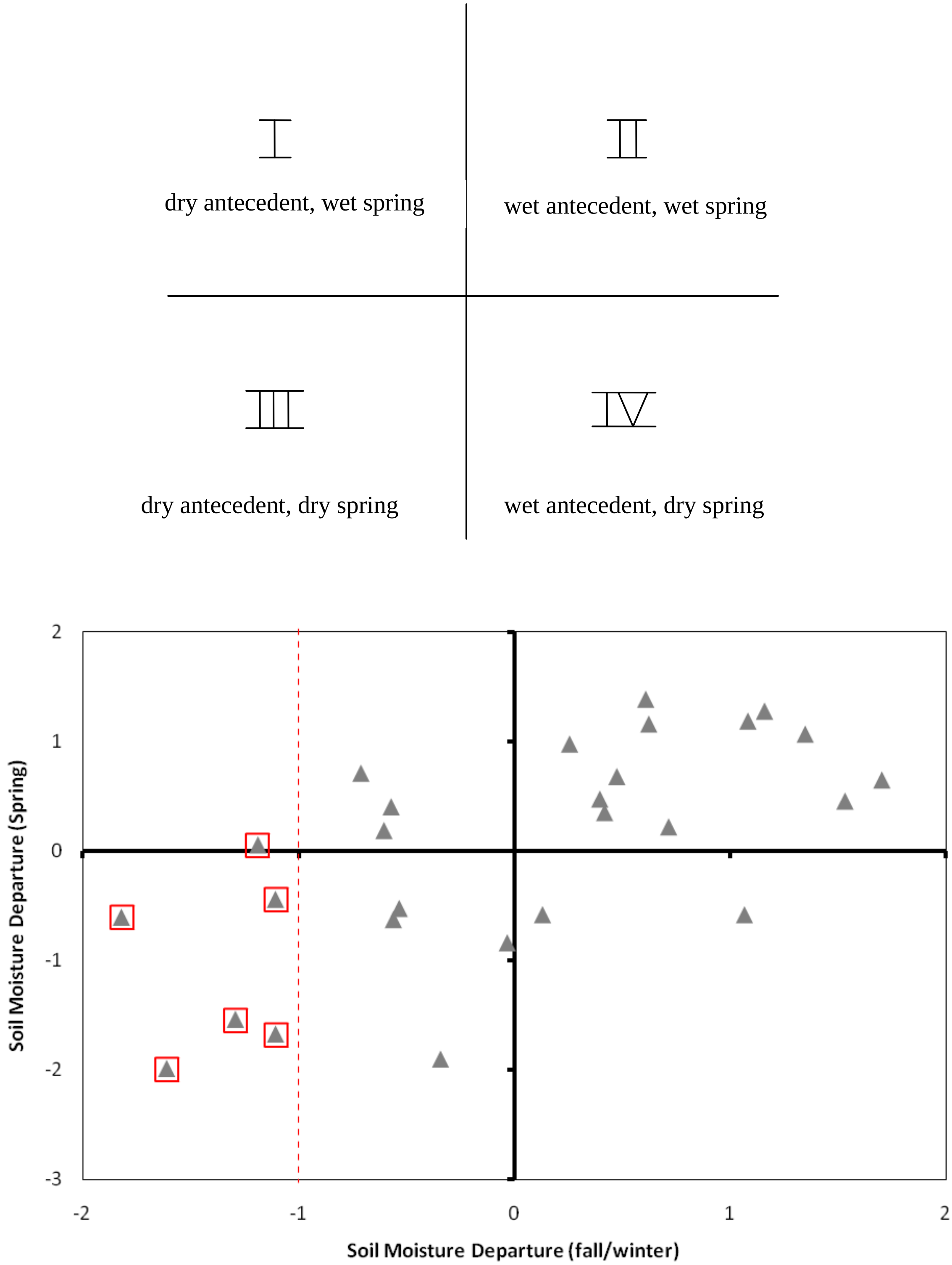

Fig. 4.15. (a) Labeled quadrants for interpretation of scatterplot and (b) scatterplot of 6-month antecedent soil moisture (x-axis) and spring soil moisture (y-axis). Drought years are outlined in red.

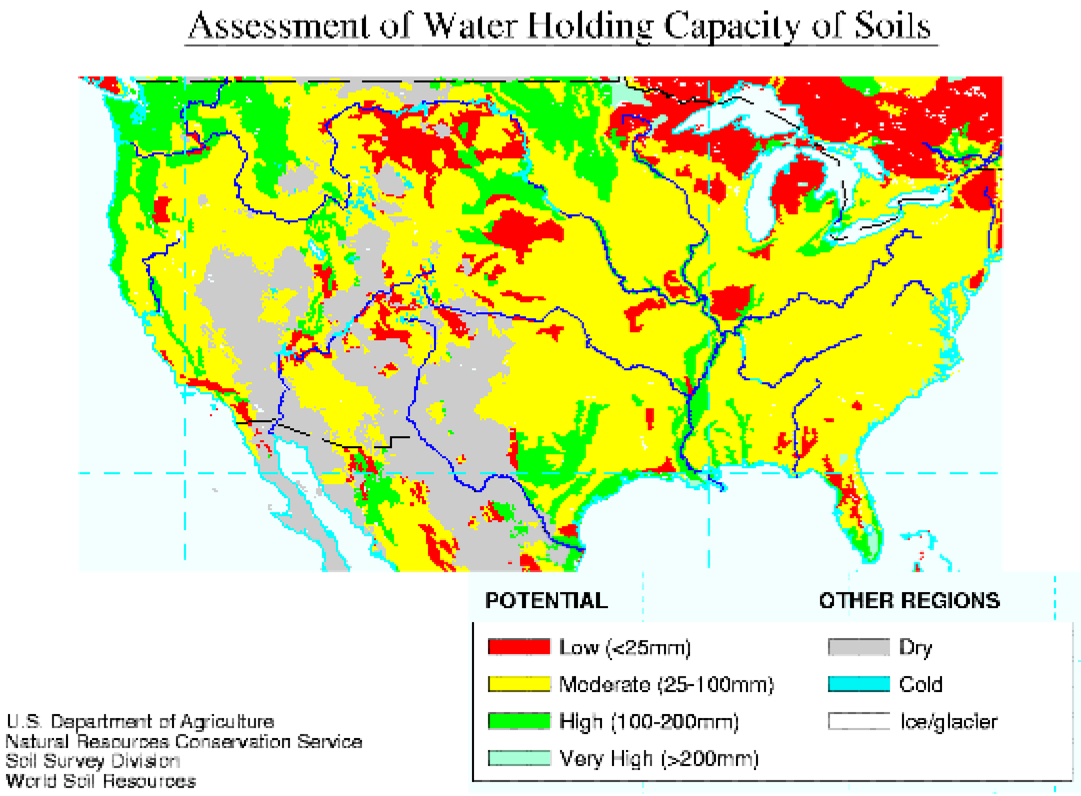

Fig. 4.16. Potential water holding capacity of soils in the U.S. Southeastern United States soils typically hold 25-100 mm of water.

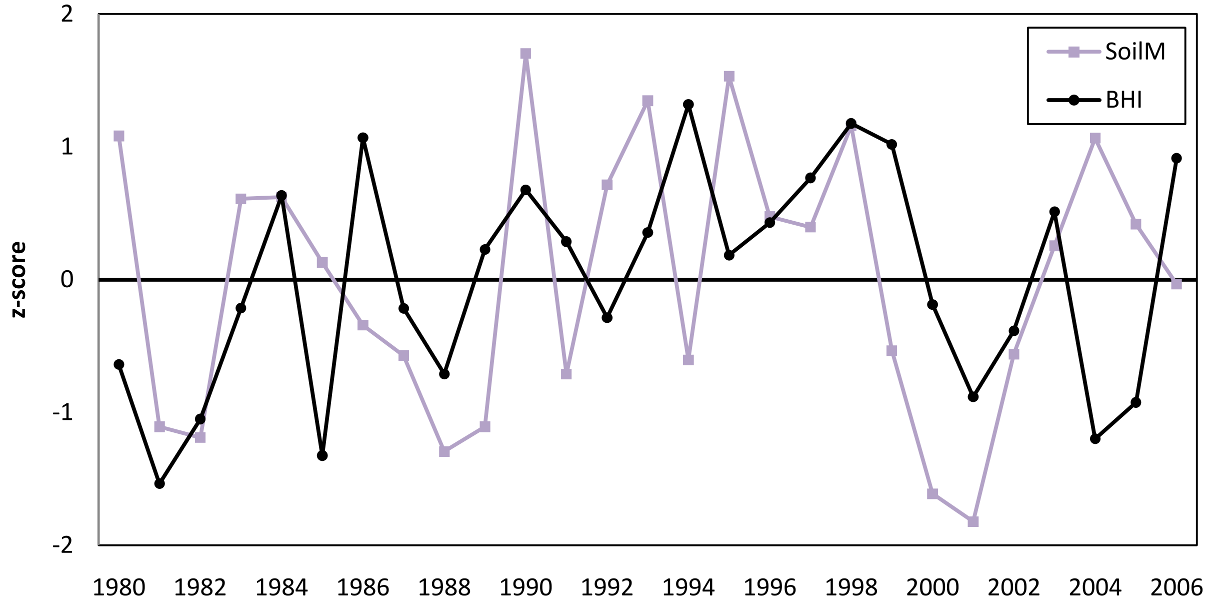

Fig. 4.17. Time series of the 6-month antecedent BHI (black) and 6-month normalized soil moisture (purple) area-averaged over the domain.

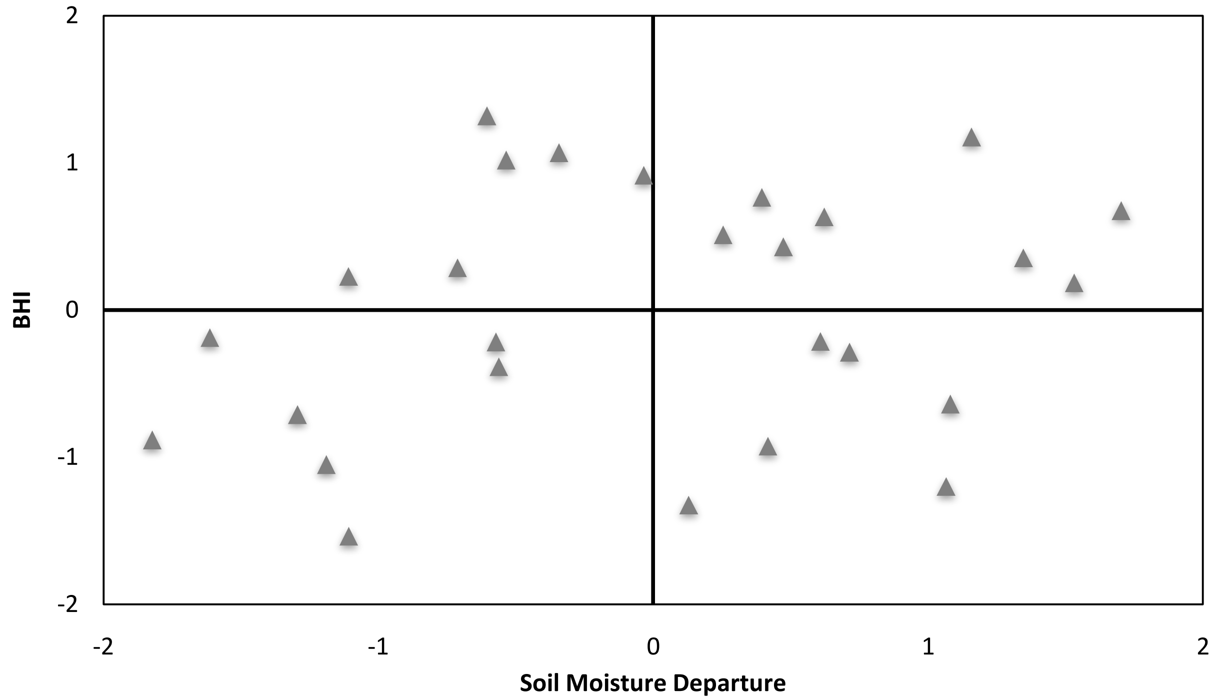

Fig. 4.18. Scatterplot of the 6-month antecedent BHI and 6-month normalized soil moisture area-averaged over the domain. There is not a significant positive correlation between the two variables at the 95% confidence level (R = 0.25).

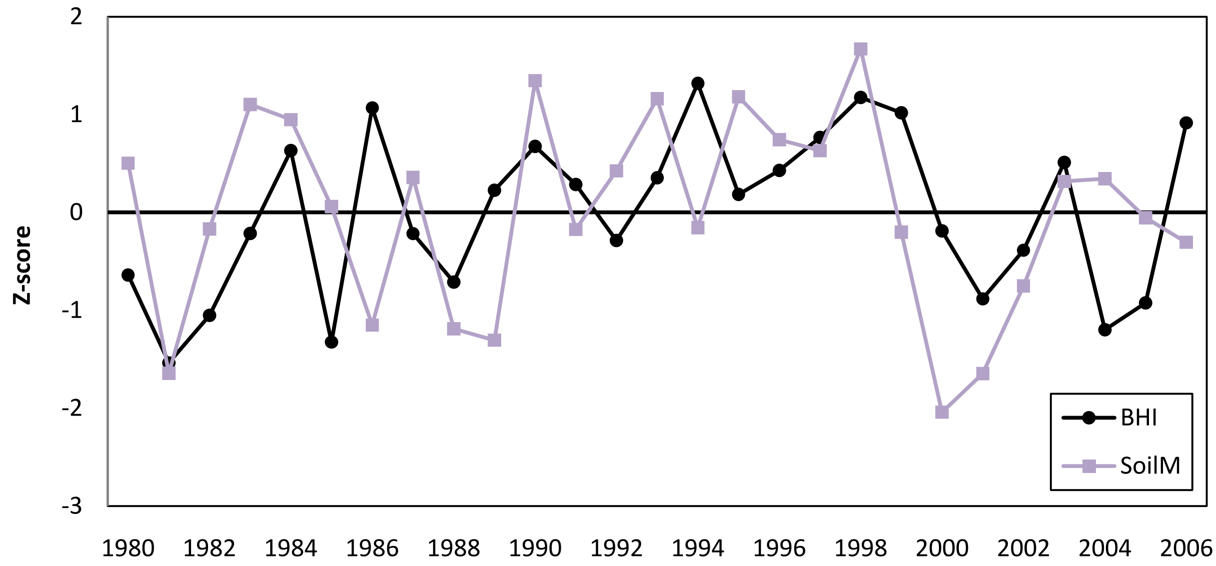

Fig. 4.19. Time series plot of 6-month antecedent BHI (black) and 1-month antecedent normalized soil moisture (purple).

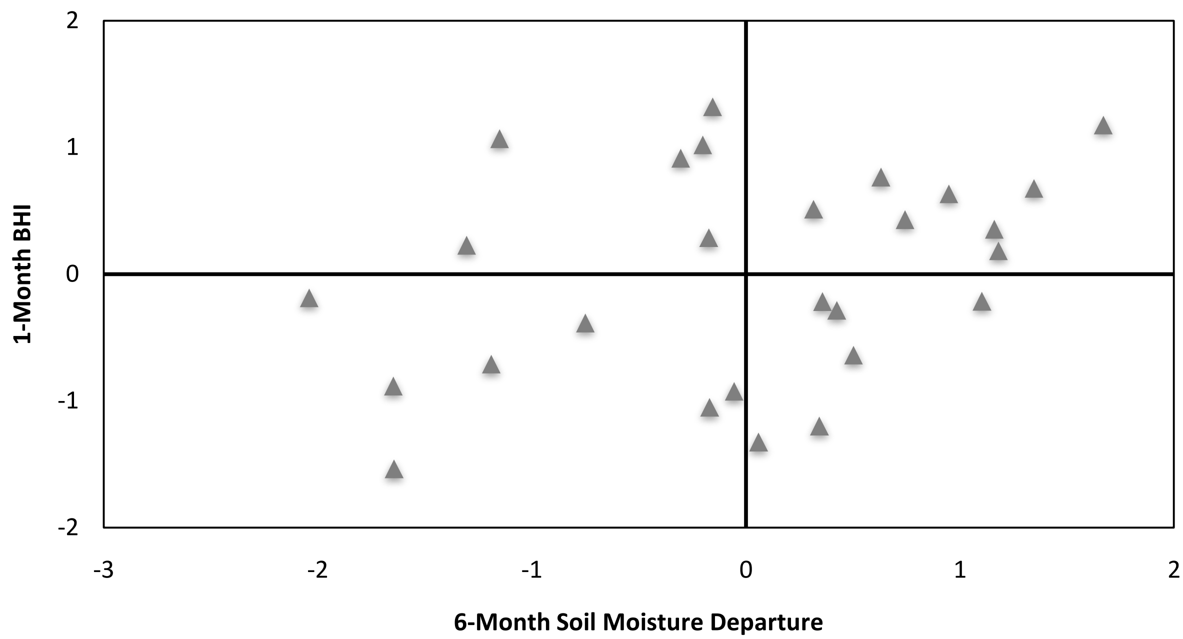

Fig. 4.20. Scatterplot of 6-month antecedent BHI and 1-month antecedent normalized soil moisture. The T-Test indicates there is a significant positive correlation at the 95% confidence level ($R = 0.34$).

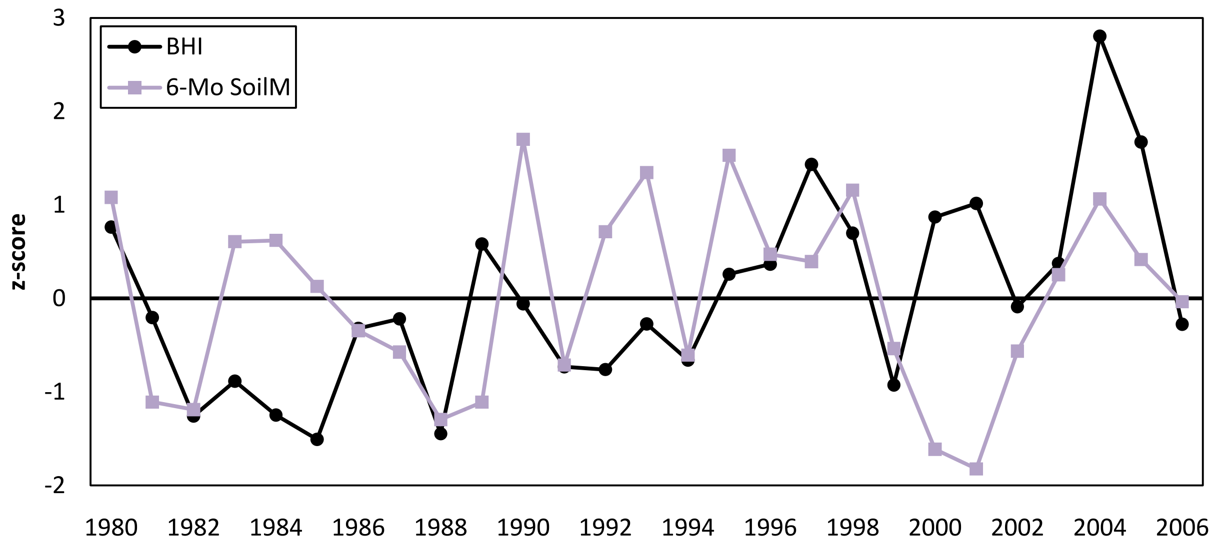

Fig. 4.21. Time series of warm season BHI (black) versus 6-month antecedent normalized soil moisture (purple).

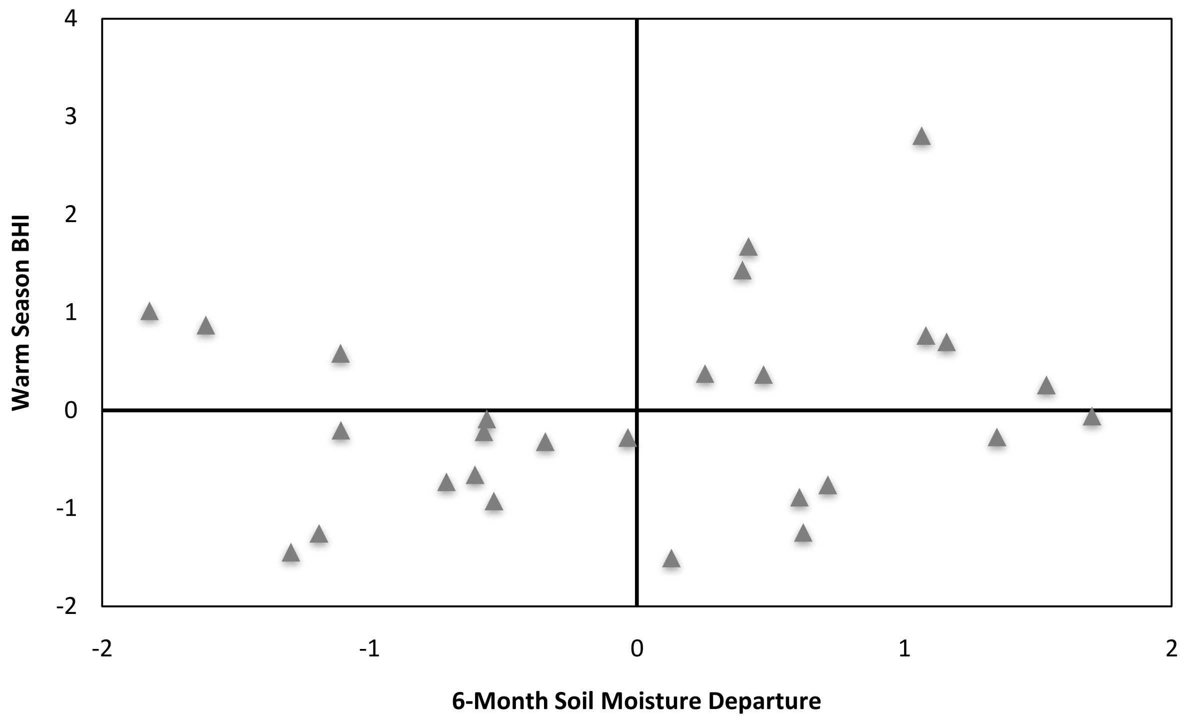

Fig. 4.22. Scatterplot of warm season BHI versus 6-month antecedent normalized soil moisture. There is not a significant positive correlation (R = 0.20).

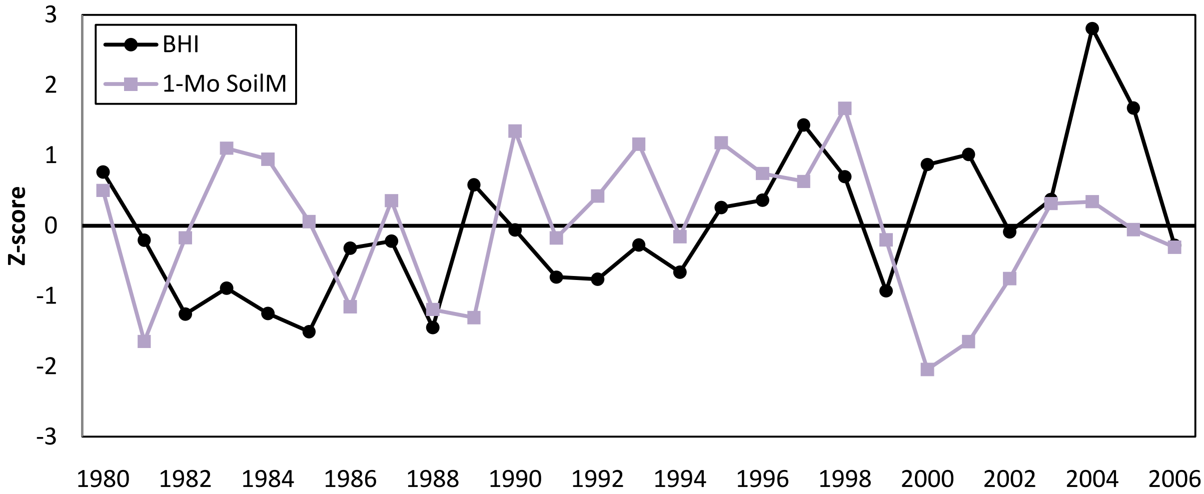

Fig. 4.23. Time series of warm season BHI (black) and 1-month antecedent normalized soil moisture (purple).

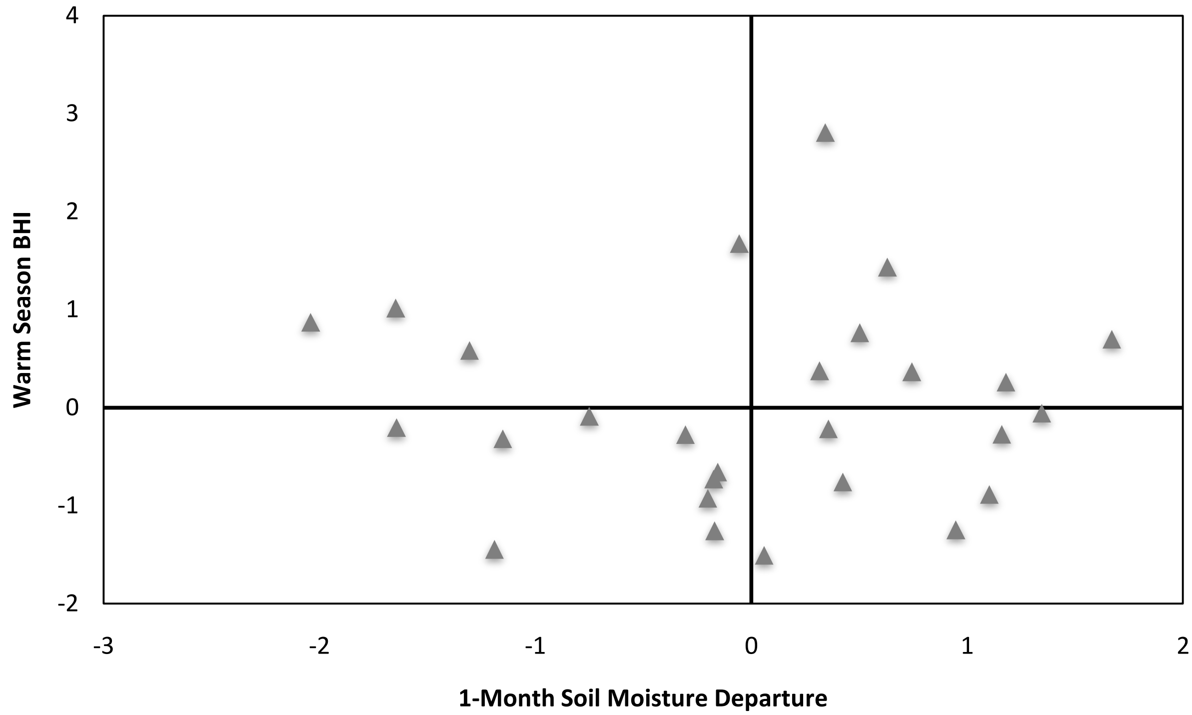

Fig. 4.24. Scatterplot of warm season BHI versus 1-month antecedent normalized soil moisture. There is no correlation between the two datasets (*R* = 0.00).

CHAPTER 5

CONCLUSIONS

5.1 Summary

Soil moisture interacts with the atmosphere through moisture and energy exchanges between the surface and planetary boundary layer. The lack of sufficient soil moisture during the fall/winter is hypothesized to reduce convective development and tornadoes in the spring as part of a soil moisture memory effect. The IPCC has indicated the probability of an increase in extreme events and acceleration of the water cycle due to climate change (Shepherd et al. 2009), which has implications for drought-convection feedbacks. The consensus on soil moisture – atmospheric feedbacks is that moisture gradients influence convective development leading to storms. However, very little literature exists on the extension of this feedback to convective hazards such as tornado activity. Galway (1979) found high-precipitation years tend to have more tornadoes than low-precipitation years, but he did not find that tornadoes are suppressed under drought conditions. However, the datasets Galway used are now outdated and spanned a time period when tornado counts were underestimated due to sparse populations and lack of Doppler radar networks. A recent study by Shepherd et al. (2009) suggests tornado activity in the spring is suppressed in north Georgia when meteorological drought occurred the previous fall. The large-scale water-cycle hazards associated with climate change have significant implications for rainfall patterns and future droughts, making it imperative to perform a climatological analysis on related feedbacks. The research presented herein has provided a better understanding of the relationship between the intensity of spring tornado activity and antecedent drought conditions in the southeastern United States. The following sections describe the major findings, conclusions, and future directions of the thesis.

5.2 Major Findings

The major findings of this thesis are:

- The 6-month normalized soil moisture most consistently correlates with the PDSI *Z*-index 1980-2006, as compared with the 1-month and 2-month soil moisture.
- Normalized soil moisture and tornado days have a moderate positive correlation. Drought years are strongly associated with equal to or below normal tornado days while non-drought years are associated with both above and below normal tornado days. This result continues to affirm the possibility that there is some seasonal predictive capacity for tornado days when the previous fall and winter are experiencing drought.
- Tornado track composite maps suggest fewer tornadoes occur over the study area during drought years than non-drought years.
- Tornado seasons preceded by drought lack violent tornadoes (F4 and F5) and have shorter, narrower tornado tracks compared to seasons preceded by wet fall/winter.
- 6-month antecedent drought conditions correspond to lower February CAPE values (higher CIN) over most of the study area as compared to non-drought conditions. Correlation analysis shows below normal soil moisture results in lower CAPE while above normal soil moisture does not seem to show any trend.
- There is a small difference in large-scale synoptic patterns between drought and non-drought cases, as defined by the 500 hPa geopotential heights. The drought composite shows some ridging, which may be a factor in fall/winter soil moisture lingering into spring.
- Six-month antecedent drought periods correspond to the driest spring soil moisture regimes, while dry to normal years correspond to either dry or wet springs. The wettest antecedent periods are associated with wet springs. The results offer one of the first quantitative assessments of a physical mechanism, namely soil moisture memory and persistence that can describe why drought in the previous fall/winter appears to be a predictor of below normal tornado days.

- The Bermuda High during the fall/winter may have some influence on the soil moisture conditions during the same period, but there is non statistically-significant relationship. The warm season BHI does not have any significant correlation to the following fall/winter drought and can not be viewed as a predictor.

5.3 Conclusions

This research suggests that soil moisture content provides an adequate measure of drought conditions in the southeastern United States, and may be utilized in future studies. Use of soil moisture alone to assess drought is spatially and temporally more compatible with current and future satellite and in-situ datasets. Anomalously high pressure over Bermuda in the fall/winter tends to coincide with drought conditions, although the correlation is not significant and factors influencing drought should be further explored.

Correlation analysis indicates drought conditions during September-February are associated with drought conditions in the spring, reduced CAPE, enhanced CIN, and below normal tornado activity. Anomalously wet soils during September- February are associated with wet conditions in the spring, enhanced CAPE, reduced CIN, but no correlation to tornado activity. Soil moisture memory is suggested as the possible physical mechanism linking fall/winter drought to spring tornado activity. When drought occurs in September-February, the soil moisture conditions tend to persist into the spring. This lack of soil moisture reduces surface moisture transport to the planetary boundary layer, thus removing one of the key ingredients for storm and tornado development. However, as seen with the 14 March 2008 tornado in Atlanta, heavy rainfall events during drought conditions may dominate soil moisture memory and enhance tornado activity potential. This hypothesis is beyond an observational study and is currently being investigated from a modeling approach at Purdue University.

5.4 Future Directions

Research presented in this paper has implications for soil moisture feedbacks and tornado forecasting. Hurricane seasons can be predicted on a long-lead scale by knowing the QBO Phase, ENSO, and Sahelian rainfall. Likewise, tornado season intensity may also be predicted through analyzing drought conditions. During an average year, there are 800 tornado reports nationwide, 80 tornado-related deaths and 1,500 injuries (NOAA NWS 2010). The 14 March 2008 tornado in Atlanta raised awareness of extreme weather events and suggests further research on soil moisture-tornadic feedbacks. Surface-forced convection is not the only scenario for tornadoes to form, so this research only proposes a potential guide for likelihood of tornadic activity in the spring. Future studies may investigate soil moisture memory in more depth, as the results of this research show a striking persistence from fall/winter into spring.

REFERENCES

Alonge, C. J., K. I. Mohr, and W-K Tao, 2006: Numerical studies of wet versus dry soil regimes in the West African Sahel. *J. Hydrometeor*., **8**, 102-116.

Andreadis, K. M., et al., 2005: Twentieth-century drought in the coterminous United States. *J. Hydrometeor*., **6**, 985-1001.

Anthes, R. A., 1983: Enhancement of convective precipitation by mesoscale variations in vegetative covering in semiarid regions. *J. Climate Appl. Meteor*., **23**, 541-554.

Ashley, W. S., 2007: Spatial and temporal analysis of tornado fatalities in the United States: 1880-2005. *Wea. Forecasting*, **22**, 1214-1228.

Bosilovich, M. G., and S. D. Schubert, 2001: Precipitation recycling over the central United States diagnosed from the GEOS-1 Data Assimilation System. *J. Hydrometeor*., **2**, 26-35.

Bosilovich, M. G., and W.-Y. Sun, 1998: Numerical simulation of the 1993 midwestern flood: land atmosphere interactions. *J. Climate*, **12**, 1490-1505.

Bove, M. C., 1998: Impacts of ENSO on United States tornado activity. Preprints, *19th Conf. on Severe Local Storms*, Minneapolis, MN, Amer. Meteor. Soc., 313-316.

Bunkers, M. J., B. A. Klimowski, and J. W. Zeitler, 2002: The importance of parcel choice and the measure of vertical wind shear in evaluating the convective environment. Preprints, *21st Conf. on Severe Local Storms*, San Antonio, TX, Amer. Meteor. Soc., 379–382.

Bunkers, M. J., J. R. Wetenkamp, J. J. Schild, and A. Fischer, 2009: Observations of the relationship between 700-mb temperatures and severe weather reports across the contiguous United States. *Wea. Forcasting*, submitted.

Chang, J.-T. and P. Wetzel, 1990: Effects of spatial variations of soil moisture and vegetation on the evolution of a prestorm environment: A numerical case study. *Mon. Wea. Rev.*, **119,** 1368-1390.

Chen, F., and R. Avissar, 1994: Impact of land-surface moisture variability on local shallow convective cumulus and precipitation in large-scale models. *J. Appl. Meteor*., **33**, 1382-1401.

Clark, C. A., and R. W. Arrit, 1995: Numerical simulations of the effect of soil moisture and vegetation cover on the development of deep convection. *J. Appl. Meteor.,* **34**, 2029-2045.

Cook, A. R., and J. T. Schaefer, 2008: The relation of El Niño-Southern Oscillation (ENSO) to winter tornado outbreaks. *Mon. Wea. Rev*., **136**, 3121-3137.

Dai, A., K. E. Trenberth, and T. Qian, 2004: A global dataset of Palmer Drought Severity Index for 1870 2002: Relationship with soil moisture and effects of surface warming. *J. Hydrometeor*., **5**, 1117-1130.

Dirmeyer, P. A., C. A. Schlosser, and K. L. Brubaker, 2008: Precipitation, recycling and land memory: An integrated analysis. COLA Tech. Rep. 257, 24 pp.

Doswell III, C. A., and D. W. Burgess, 1987: On some issues of United States tornado climatology. *Mon. Wea. Rev*., **116**, 495-501.

Doublin, J. K., and A. J. Grundstein, 2008: Warm-season soil-moisture deficits in the southern United States. *Phys. Geog*., **29**, 3-18.

Douville, H., S. Conil, S. Tyteca, and A. Voldoire, 2007: Soil moisture memory and West African monsoon predictability: artefact or reality? *Clim. Dyn*., **28**, 723-742.

Dracup, J. A., K. S. Lee, and E. G. Paulson, Jr., 1980: On the definition of droughts. *Water Resources Res*., **16**, 297-302.

Eltahir, E. A. B, and R. L. Bras, 1996: Precipitation recycling. *Rev. Geophys*., **34**, 367-378.

Frates, M. J., 2010: Demystifying colloquial tornado alley-delineation of new “tornado alleys” in the United States. Poster Presentation. 2010 AAG Washington, D.C.

Frye J. D., and T. L. Mote, 2010: The synergistic relationship between soil moisture and the low-level jet and its role on the pre-storm environment in the southern Great Plains. *J. Appl. Meteor. Climatol*., **49**, 775-791.

Gallus, W. A., and M. Segal, 2000: Sensitivity of forecast rainfall in a Texas convective system to soil moisture and convective parameterization. *Wea. Forecasting*, **15**, 509-525.

Galway, J. G., 1979: Relationship between precipitation and tornado activity. *Water Resources Res*., **15**, 961-964.

Grazulis, T. P., 1993: *Significant Tornadoes, 1680-1991*. Environmental Films, 1326 pp.

Hagemeyer, B. C., 1998: Significant extratropical tornado occurrences in Florida during strong El Niño and strong La Niña events. Preprints, *19th Conf. on Severe Local Storms,* Minneapolis, MN, Amer. Meteor. Soc., 412-415.

Hanesiak, J. M., R. L. Raddatz, and S. Lobban, 2004: Local initiation of deep convection on the Canadian prairie provinces. *Bound.-Layer Meteor*., **110**, 455-470.

Hanesiak J., A. Tat and R. Raddatz, 2009: Initial soil moisture as a predictor of subsequent severe summer weather in the cropped grassland of the Canadian Prairie provinces. *Int. J. Climatol*., **29**, 899–909.

Henderson, K. G., and A. J. Vega, 1996: Regional precipitation variability in the southeastern United States. *Phys. Geography*, **17**, 93-112.

Holton, J. R., 2004: *An Introduction to Dynamic Meteorology*. Vol. 88, *International Geophysics Series,* Elsevier Inc., 535 pp.

Hong, X., M. J. Leach, and S. Raman, 1995: A sensitivity study of convective cloud formation by vegetative forcing with different atmospheric conditions. *J. Appl. Meteor.*, **34**, 2008-2028.

Iwasaki, H., et al, 2008: Diurnal variation of convective activity and precipitable water around Ulaanbaator, Mongolia, and the impact of soil moisture on convective activity at nighttime. *Mon. Wea. Rev*., **136**, 1401-1415.

Jiang, X., G.-Y. Niu, and Z.-L. Yang, 2009: Impacts of vegetation and groundwater dynamics on warm season precipitation over the central United States. *J. Geophys. Res*., **114**, 1-15.

Karl, T. R., and R. G. Quayle, 1981: The 1980 Summer heat wave and drought in historical perspective. *Mon. Wea. Rev*., **109**, 2055–2073.

Karl, T. R., and P. J. Young, 1987: The 1986 Southeast drought in historical perspective. *Bull. Amer. Meteor. Soc*., **68**, 773-778.

Keyantash, K., and J. A. Dracup, 2002: The quantification of drought: An evaluation of drought indices. *Bull. Amer. Meteor. Soc*., **83**, 1167-1180.

Kim, Y., and G. Wang, 2007: Impact of initial soil moisture anomalies on subsequent precipitation over North America in the coupled land-atmosphere model CAM3-CLM3. *J. Hydrometeor*., **8**, 513-533.

Lanicci, J. M., T. N. Carlson, and T. T. Warner, 1987: Sensitivity of the Great Plains severe-storm environment to soil-moisture distribution. *Mon. Wea. Rev*., **115**, 2660-2673.

Lemon, L. R., and C. A. Doswell III, 1979: Severe thunderstorm evolution and mesocyclone structure related to tornadogenesis. *Mon. Wea. Rev*., **107**, 1184-1197.

Lynn, B. H., W.-K. Tao, and P. Wetzel, 1998: A study of landscape –generated deep moist convection. *Mon. Wea. Rev*., **126**, 928-942.

Meng, L., 2009: Examining the relationship between antecedent soil moisture and summer precipitation in the U.S. Great Plains. Ph.D dissertation, Texas A&M University, 130 pp.

Munoz, E., and D. Enfield, 2009: The boreal spring variability of the Intra-Americas low-level jet and its relation with precipitation and tornadoes in the eastern United States. *Clim. Dyn*., In Press, doi:10.1007/s00382-009-0688-3.

NARR, cited 2010: North American Regional Reanalysis Homepage [Available online at http://www.emc.ncep.noaa.gov/mmb/rreanl/]

NOAA NWS, cited 2010: A preparedness guide including safety information for schools. [Available online at http://www.nssl.noaa.gov/edu/safety/tornado.pdf]

Oglesby, R. J., S. Marshall, D. J. Erickson III, J. O. Roads, and F. R. Robertson, 2002: Thresholds in atmosphere-soil moisture interactions: Results from climate model studies. *J. Geophys. Res*., **107**, 4224, doi:10.1029/2001JD001045.

Pal, J. S., and E. A. B. Eltahir, 2001: Pathways relating soil moisture conditions to future summer rainfall within a model of the land-atmosphere system. *J. Climate*, **14**, 1227-1242.

Pan, Z., E. Takle, M. Segal, and R. Turner, 1996: Influences of model parameterization schemes on the response of rainfall to soil moisture in the central US. *Mon. Wea. Rev*., **124**, 1786-1802.

Quiring, S. M., 2009: Developing objective operational definitions for monitoring drought. *J. Appl. Meteor. Climatol*., **48**, 1217-1229, doi:10.1175/2009JAMC2088.1.

Rabin, R. M. S. Stadler, P. J. Wetzel, D. J. Stensrud, and M. Gregory, 1990: Observed effects of landscape variability on convection clouds. *Bull. Amer. Met. Soc.*, **71**, 272-280.

Raddatz R. L. and J.D. Cummine, 2003: Inter-annual variability of moisture flux from the prairie agro-ecosystem: impact of crop phenology on the seasonal pattern of tornado days. *Bound.-Layer Meteor*., **106**, 283–95.

Salby, M. L., 1996: *Fundamentals of Atmospheric Physics*. Vol. 61, *International Geophysics Series*, Academic Press, 627 pp.

Segal, M., R. W. Arritt and C. Clark, 1995: Scaling evaluation of the effect of surface characteristics on potential for deep convection over uniform terrain. *Mon. Wea. Rev*., **123**, 383-400.

Shepherd, M., D. Niyogi, and T. Mote, 2009: A seasonal-scale climatological analysis correlating spring tornado activity with antecedent fall-winter drought in the Southeastern United States. *Env. Res. Lett*., **4**, 24012, doi:10.1088/1748-9326/4/2/024012.

da Silva, R. R., and R. Avissar, 2006: The hydrometeorology of a deforested region of the Amazon basin. *J. Hydrometeor*., **7**, 1028-1042.

Trenberth, K. E. et al., 2007: Observations: Surface and atmospheric climate change. In: *Climate Change 2007: The Physical Science Basis. Contribution of Working Group I to the Fourth Assessment Report of the Intergovernmental Panel on Climate Change* [Solomon, S., D. Qin, M. Manning, Z. Chen, M. Marquis, K.B. Averyt, M. Tignor and H.L. Miller (eds.)]. Cambridge University Press, Cambridge, United Kingdom and New York, NY, USA.

Trier, S. B., F. Chen, and K. W. Manning, 2004: A study of convection initiation in a mesoscale model using high-resolution land surface initial conditions. *Mon. Wea. Rev*., **132**, 2954-2976.

Wallace, J. M., and P. V. Hobbs, 2006: *Atmospheric Science.* 2nd ed. Elsevier Inc., 483 pp.

Wilhite, D. A., and M. H. Glantz, 1985: Understanding the drought phenomenon: The role of definitions. *Water Intl.*, **10**, 111–120.

Williams, E., and N. Renno, 1993: An analysis of the conditional instability of the tropical atmosphere. *Mon. Wea. Rev*., **121**, 21-36.

Wu, W., and R. E. Dickinson, 2004: Time scales of layered soil moisture memory in the context of land atmosphere interactions. *J. Climate,* **17**, 2752-2764.

Wu, W., R. E. Dickinson, H. Wang, Y. Liu, and M. Shaikh, 2007: Covariabilities of spring soil moisture and summertime United States precipitation in a climate simulation. *Int. J. Climatol*., **27**, 429-438.

Zheng, X., and E. A. B. Eltahir, 1998: The role of vegetation in the dynamics of West African monsoons. *J. Climate*, **11**, 2078-2096.